

---

# Incidence Networks for Geometric Deep Learning

---

**Marjan Albooyeh\***

Department of Computer Science  
University of British Columbia  
Vancouver, BC V6T1Z4, Canada  
albooyeh@cs.ubc.ca

**Daniele Bertolini\***

dbertolini84@gmail.com

**Siamak Ravanbakhsh**

Department of Computer Science  
University of British Columbia  
Vancouver, BC V6T1Z4, Canada  
siamakx@cs.ubc.ca

## Abstract

One may represent a graph using both its node-edge and its node-node incidence matrices. This choice of representation leads to two classes of equivariant neural networks for attributed graphs that we call incidence networks. Moving beyond graphs, incidence tensors can represent higher dimensional geometric data structures, such as attributed mesh and polytope. For example, a triangulated mesh can be represented using either a “homogeneous” node-node-node or an “inhomogeneous” node-edge-face incidence tensor. This is analogous to the choice of node-node vs. node-edge in graphs. We address the question of “which of these combinations of representation and deep model is more expressive?” and prove that for graphs, homogeneous and inhomogeneous models have equal expressive power. For higher dimensional incidence tensors, we prove that the inhomogeneous model, which is simpler and more practical, can also be more expressive. We demonstrate the effectiveness of incidence networks in quantum chemistry domain by reporting state-of-the-art on QM9 dataset, using both homogeneous and inhomogeneous representations.

## 1 Introduction

Many interesting data structures have alternative yet equivalent tensor representations. For example, we can represent simple graphs using both *homogeneous* node-node and *inhomogeneous* node-edge incidence matrices.<sup>2</sup> We use H-MATRIX and I-MATRIX as their abbreviation in the following. In addition to graphs, incidence tensors can express other important mathematical structures, motivating the family of *incidence networks* that operate on these tensor representations. To design these networks, one has to choose one of the two representations (H-TENSOR or I-TENSOR) and create a neural layer “suitable” for that representation. We define suitability of the neural layer using the notion of *equivariance*. Equivariance provides a useful inductive bias for constructing functions on structured domains by constraining the output of a functions  $f : \mathcal{X} \rightarrow \mathcal{Y}$  under particular transformations  $g \in G$  of the input, such that

$$f(g \cdot x) = g \cdot f(x) \quad \forall x \in \mathcal{X}, g \in G, \quad (1)$$

---

\*equal contributions.

<sup>2</sup>While one may also consider edge-edge incidence matrix, there are pathological cases where two different graphs share the same edge-edge incidence matrix.

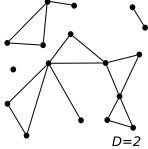
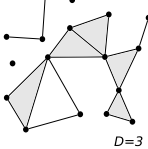
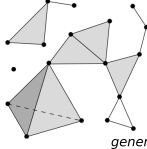
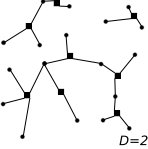
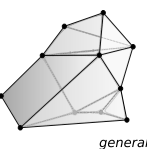
	a. Undirected Graph	b. Triangulated Mesh	c. Simplicial complex	d. Hyper-Graph	e. Mesh/Polytope
					
	$D=2$	$D=3$	general $D$	$D=2$	general $D$
Inhom.	$17_{\text{nodes}} \times 18_{\text{edges}}$ 4 params.	$17_{\text{nodes}} \times 21_{\text{edges}} \times 5_{\text{faces}}$ 8 params.	$\#0\text{-dim} \times \dots \times \#(D-1)\text{-dim faces}$ $2^D$ params.	$17_{\text{nodes}} \times 18_{\text{edges}}$ 4 params.	$\#0\text{-dim} \times \dots \times \#(D-1)\text{-dim faces}$ $2^D$ params.
Hom.	$17_{\text{nodes}} \times 17_{\text{nodes}}$ 9-15 params.	$17_{\text{nodes}} \times 17_{\text{nodes}} \times 17_{\text{nodes}}$ 23-203 params.	$\#\text{nodes} \times \dots \times \#\text{nodes}$ $(2D^3 + 9D^2 + D)/6$ or Bell( $2D$ ) params.		

Figure 1: Examples of geometric structures with incidence tensor representation. (a),(b) and (c) have both homogeneous (H-TENSOR) and inhomogeneous (I-TENSOR) representations, where one may assign attributes to faces of different dimensions. (d) (symmetric) hyper-graphs, in which the nodes adjacent to a hyper-edge are order-less are best represented using node-edge incidence matrix. (e) Similarly, a polytope or a general mesh, in which a face may be adjacent to arbitrary number of faces of lower dimensions, is best represented in an inhomogeneous form; see Appendix C. H-TENSOR for all of these structures is *strongly symmetric* and the two parameters indicate the effect of our choice in maintaining this symmetry at the output of the H-LAYER.

where  $g \cdot x$  is a “consistently” defined transformation of  $x$  parameterized by  $g \in G$ . For example, in a convolution layer,  $G$  is the group of discrete translations, and (1) means that any translation of the input leads to the same translation of the output. When  $f : x \mapsto \sigma(\mathbf{W}x)$  is a standard feed-forward layer and  $G$ -action is discrete, the equivariance property of (1) can be imposed by tying the elements of the weight matrix  $\mathbf{W}$  (Ravanbakhsh et al., 2017).

The H-MATRIX and I-MATRIX can both represent the same underlying graph with node and edge attributes, but they have different symmetries: we may permute the rows and columns of H-MATRIX using an arbitrary permutation, as long as the same permutation is applied to the rows and columns. In contrast, independent shuffling of rows and columns is allowed in an I-MATRIX. In both cases the underlying graph remains the same. The corresponding parameter-sharing in  $\mathbf{W}$  is therefore different, with H-MATRIX requiring a larger number of parameters.

We prove that the equivariant (linear) layers for H-MATRIX and I-MATRIX representation of a graph span the same feature space, up to doubling the number of layers. We show comparable results between the two models in our experiments which also establishes their state-of-the-art performance on one of the largest graph datasets. We then show that this parallel between homogeneous and inhomogeneous representation extends to higher dimensional geometric structures; see Fig. 1. For example, an attributed triangulated mesh has a node-node-node homogeneous tensor representation (H-TENSOR) as well as an inhomogeneous node-edge-face tensor expression (I-TENSOR). The question becomes *which representation and deep model should one use?* To answer this, we use a novel interpretation of parameter-sharing for homogeneous tensors in terms of pooling and broadcasting over “hyper-diagonals” of the tensor. This allows us to prove that in higher dimensions (beyond graphs), using the I-TENSOR representation leads to a more expressive equivariant layer. Combined with its ease of implementation, this makes a case for using inhomogeneous representation, especially when dealing with symmetric (or undirected) geometric objects, such as mesh and polytope. Table 1 summarizes our findings.

## 2 Related Works

Deep learning with structured data is a very active area of research; see (Battaglia et al., 2018; Hamilton et al., 2017). Our work relates to deep models of graph (and mesh) as well as a body of work on equivariant deep learning. Graph neural networks go back to Scarselli et al. (2009), who introduced a general iterative framework for learning neural functions on graphs. More recently, (Gilmer et al., 2017) proposed to learn iterative updates of messages that are exchanged between nodes in a graph. This framework generalizes several other graph neural architectures (Li et al., 2015; Duvenaud et al., 2015; Kearnes et al., 2016; Schütt et al., 2017), including the spectral methods that we discuss later. Covariant compositional network (CCN) of Kondor et al. (2018) further extends the message passing framework by considering basic tensor operations that preserve equivariance.

Table 1: A summary of comparison between homogeneous vs. inhomogeneous incidence networks.

			RELATIVE	EXPRESSIVENESS	UNIQUE	LINEAR	CHANNELS
			EASE OF USE		PARAMETERS	LAYERS	
GRAPH	UNDIRECTED	HOM.	✓	=	9	$\geq 1$	$\times 1$
		INHOM.	✓✓	=	4	$\geq 2$	$\times 2$
	DIRECTED	HOM.	✓	=	15	$\geq 1$	$\times 1$
		INHOM.	✓✓	=	4	$\geq 2$	$\times 6$
$D \gtrsim 3$	SYM.	HOM.	✗	LESS	$\frac{1}{6}(2D^3 + 9D^2 + D)$	$\geq 1$	$\times 1$
		INHOM.	✓✓	MORE	$2^D$	$\geq 2$	$\times D$
	ASYM.	HOM.	✗	LESS	$\text{Bell}(2D)$	$\geq 1$	$\times 1$
		INHOM.	✗	MORE	$2^D$	$\geq 2$	$\times \alpha(D)^4$

While the resulting architecture can be quite general, it comes at the cost of efficiency<sup>3</sup> Most directly related to this paper are the equivariant models of [Hartford et al. \(2018\)](#) for interactions across sets, and the equivariant graph networks of [Maron et al. \(2018\)](#). We revisit both of these models in the following sections. [Graham & Ravanbakhsh \(2019\)](#) further generalize these two types of equivariant linear layers to multi-relation setting. [Maron et al. \(2019\)](#) recently showed the universality of such invariant neural networks.

A different body of work in geometric deep learning extend convolution to graphs using the spectrum of the graph Laplacian ([Bronstein et al., 2017](#); [Bruna et al., 2014](#)). While principled, in its complete form, the Fourier bases extracted from the Laplacian are instance dependent and lack of any parameter or function sharing across the graph limits their generalization. Following ([Henaff et al., 2015](#); [Defferrard et al., 2016](#)), [Kipf & Welling \(2016\)](#) propose a single-parameter simplification of spectral method that addresses this limitation. Interestingly this minimal graph convolution model can also be derived from neural message passing, as well as through simplification of equivariant graph networks.

### 3 Incidence Networks for Graphs

For the benefit of clarity, and without loss of generality, in the following we assume the attribute graph  $\mathfrak{G} = ([N], \mathcal{E} \subseteq [N] \times [N])$  for  $N = \{0, \dots, N-1\}$  is fully connected. We assume the node-features are encoded in the edge-features for the self-loop  $e = (n, n), n \in [N]$ . The H-TENSOR representation  $\mathbf{X} \in \mathbb{R}^{N \times N \times K}$  uses the diagonal and off-diagonal elements to encode  $K$ -dimensional node and edge features, respectively. Alternatively we can represent the same graph using a sparse I-TENSOR  $\mathbf{Y} \in \mathbb{R}^{N \times N(N-1) \times 2K}$ , where  $N(N-1)$  is the number of edges that are not self-loop. For each node we *broadcast* its  $K$ -dimensional features across incident edges, for each edge we broadcast its  $K$ -dimensional features across its two incident nodes, for a total of  $2K$  features. Note that  $\mathbf{Y}$  has a special sparsity pattern:  $\mathbf{Y}_{nmk} \neq 0$  iff node  $n$  is incident to the edge  $m$ . In the following we assume single input and output channels  $K = 1$ ; the models trivially extend to multiple channels.

Given the I-TENSOR  $\mathbf{Y}$  of graph  $\mathfrak{G}$  with  $N$  nodes and  $N_e$  edges, we want equivariance wrt permutation of the rows and columns  $\pi \mathbf{Y} \rho$ , where  $\pi \in S_N$  and  $\rho \in S_{N_e}$  are permutation matrices, representing permutations of  $N$  and  $N_e$  objects, respectively. To achieve equivariance we need to constrain the linear map (weight tensor)  $\mathbf{A} : \mathbb{R}^{N \times N_e} \rightarrow \mathbb{R}^{N \times N_e}$ .

Assuming  $\sigma$  in (1) is a bijection, we may remove it to simplify the equivariance condition of (1):

$$\mathbf{A}(\pi \mathbf{Y} \rho) = \pi (\mathbf{A} \mathbf{Y}) \rho \quad \forall \pi, \rho \in S_N \times S_{N_e}, \mathbf{Y} \in \mathbb{R}^{N \times N_e}, \quad (2)$$

where  $\mathbf{A} \mathbf{Y}$  is understood to be the application of the linear map  $\mathbf{A}$  to the tensor  $\mathbf{Y}$  (or contraction of a tensor of type (2,2) with input tensor). This constraint further simplifies to  $\mathbf{A}_{\pi(n')\rho(m')}^{\pi(n)\rho(m)} = \mathbf{A}_{n'm'}^{nm}$ , a symmetry condition on  $\mathbf{A}$ . [Hartford et al. \(2018\)](#) show that the linear map  $\mathbf{A}$  satisfying this symmetry condition has at most 4 independent parameters, regardless of  $N$  and  $N_e$ . We call such a linear map an I-LAYER. The resulting constrained feed-forward layer  $\sigma(\mathbf{A} \mathbf{Y})$ , only adds a nonlinearity. Note

<sup>3</sup>Possibly due to the complexity of CCN architecture, experiments in [Kondor et al. \(2018\)](#) do not use all attributes in QM9 dataset and their results are not comparable to state-of-the-art.

<sup>4</sup> $\alpha(D) = \sum_{d=1}^D \sum_{m=1}^d \sum_{p=m+1}^D \binom{D}{d} \binom{d}{m} \binom{p}{m}$ .

that in contrast to (Hartford et al., 2018) we assume that input and the output of an I-LAYER have a particular sparsity pattern imposed by the incidence structure; this assumption has an important role in the proof of our theorems.

When  $\mathbf{X} \in \mathbb{R}^{N \times N}$  is an H-MATRIX, the equivariance condition of (1) for the linear map  $\mathbf{B} : \mathbb{R}^{N \times N} \rightarrow \mathbb{R}^{N \times N}$  is slightly different as we need to permute rows and columns using the same permutation

$$\mathbf{B}(\pi \mathbf{X} \pi^T) = \pi (\mathbf{B} \mathbf{X}) \pi^T \quad \forall \pi \in S_N, \mathbf{X} \in \mathbb{R}^{N \times N}. \quad (3)$$

Maron et al. (2018) show that the resulting constrained linear map  $\mathbf{B}$ , which we call an H-LAYER, only has up to 15 independent parameters, for a graph of any size.

### 3.1 Pool & Broadcast Interpretation

The I-LAYER and H-LAYER introduced above both have linear-time implementation through pooling and broadcasting that avoids matrix multiplication. Here, we formulate these for the spacial case of graphs in a way that generalizes to higher dimensional tensors. First, we need to define some new concepts.

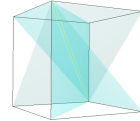
**Definition 1** (Hyper-diagonal). *hyper-diagonals of an H-TENSOR  $\mathbf{X} \in \mathbb{R}^{N \times \dots \times N \times K}$  are sub-tensors obtained by constraining some of  $n_d$  indices in  $\mathbf{X}_{n_0, \dots, n_{D-1}, k}$  to be equal. The number of hyper-diagonals of order  $D'$  is given by the Stirling number of the second kind, which counts different ways in which we can partition  $D$  labeled objects  $0, \dots, D-1$  into  $D'$  non-empty subsets  $\mathcal{D}_1, \dots, \mathcal{D}_{D'}$ . All the indices within a subset  $\mathcal{D}_i$  are then constrained to be equal, and indices within different subsets  $\mathcal{D}_i, \mathcal{D}_j, i \neq j$  are constrained to be different.*

Tensors of order  $D > 1$  have two special hyper-diagonals: 1) the main diagonal, corresponding to  $n_0 = n_1 = \dots = n_{D-1}$ ; and 2) the whole tensor excluding all other hyper-diagonals, where  $\mathcal{D}_0 = \{0\}, \dots, \mathcal{D}_{D-1} = \{D-1\}$ . A graph only has these two hyper-diagonals – i.e., diagonal and off-diagonal elements.

We now introduce our notation for pooling and broadcasting over any hyper-diagonal:

**Hyper-Pooling.**  $\text{Pool}_{\mathcal{P}, \mathcal{D}} \mathbf{X}$  extracts a hyper-diagonal associated with the tuple  $\mathcal{D}$ , and pools over a subset of its indices specified by  $\mathcal{P} \subseteq \langle 0, \dots, |\mathcal{D}| - 1 \rangle$ .  $\mathcal{D} = \langle \mathcal{D}_1, \dots, \mathcal{D}_{D'} \rangle$  is an ordered partition of the indices of  $\mathbf{X}$ , identifying a hyper-diagonal, with a particular order over its dimensions. Note that the pooled object is a tensor of order  $|\mathcal{D}| - |\mathcal{P}|$ . For example, with  $\mathbf{X} \in \mathbb{R}^{N \times N}$ ,  $\text{Pool}_{\langle 0 \rangle, \langle \{0\}, \{1\} \rangle} \mathbf{X}$ , pools over rows of matrix  $\mathbf{X}$  (excluding the diagonal), and  $\text{Pool}_{\langle \rangle, \langle \{0, 1\} \rangle} \mathbf{X}$  extracts the diagonal of matrix  $\mathbf{X}$ . For simplicity we may drop the second argument  $\mathcal{D}$  whenever the hyper-diagonal of interest is the whole tensor.

**Hyper-Broadcasting.**  $\text{Broadcast}_{\mathcal{B}, \mathcal{D}} \mathbf{X}$  broadcasts a source tensor  $\mathbf{X}$  of order  $D$  over a hyper-diagonal of a target tensor specified by the tuple  $\mathcal{D}$ , while the rest of the broadcast tensor is zero. As before,  $\mathcal{D} = \langle \mathcal{D}_1, \dots, \mathcal{D}_{D'} \rangle$  identifies a hyper-diagonal and gives a particular order over its dimensions. Since we assume  $D' \geq D$ , we need to identify  $\mathbf{X}$  with a subset of dimensions of the hyper-diagonal via another tuple  $\mathcal{B} \subseteq [D']$  with  $|\mathcal{B}| = D$ , and broadcasted across the remaining dimensions. For example, with  $\mathbf{X} \in \mathbb{R}^{N \times N}$ ,  $\text{Broadcast}_{\langle 0, 1 \rangle, \langle \{0\}, \{1\}, \{2\} \rangle} \mathbf{X}$  maps  $\mathbf{X}$  across the first two axis of a three-dimensional tensor and broadcasts its values along the third dimension.  $\text{Broadcast}_{\langle 1, 0 \rangle, \langle \{0\}, \{1\}, \{2\} \rangle} \mathbf{X} \equiv \text{Broadcast}_{\langle 0, 1 \rangle, \langle \{1\}, \{0\}, \{2\} \rangle} \mathbf{X}$  does the same operation but with the transpose of  $\mathbf{X}$ .  $\text{Broadcast}_{\langle 0, 1 \rangle, \langle \{0, 1\}, \{2\} \rangle} \mathbf{X}$  maps  $\mathbf{X}$  to a *diagonal plane* of the target tensor (Figure shows 3 diagonal planes in a tensor of order 3.) As for hyper-pooling, we may drop the second argument  $\mathcal{D}$  whenever the hyper-diagonal of interest is the whole tensor.



**I-LAYER.** The constrained linear map  $\mathbf{A}$  for an I-MATRIX has a linear-time formulation that performs pooling and broadcasting over subsets of dimensions of  $\mathbf{Y}$

$$\mathbf{A} \mathbf{Y} = \sum_{\mathcal{P} \in 2^{\{0, 1\}}} a_{\mathcal{P}} \text{Broadcast}_{\{0, 1\} - \mathcal{P}} \text{Pool}_{\mathcal{P}} \mathbf{Y}, \quad (4)$$

where  $2^{\{0, 1\}}$  is the set of all subsets of  $\{0, 1\}$ . From the notation defined above, we have dropped the hyper-diagonal index, because no hyper-diagonal is extracted beyond  $\mathbf{Y}$  itself. In this case  $\mathcal{P}$  and its

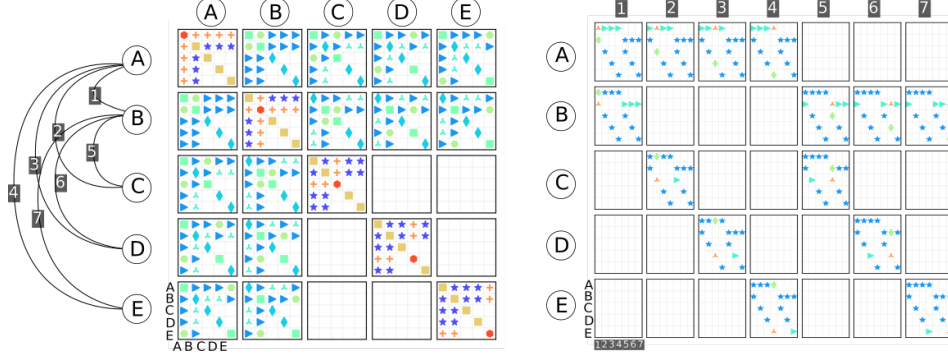


Figure 2: **(top-left)** an undirected graph with five nodes and seven edges; **(left)** parameter-sharing in the receptive field of each output unit in the homogeneous incidence network (H-LAYER). Nine unique parameters define the linear dependence of each output node and edge feature (diagonal and off-diagonal squares) on the input node and edge features (diagonal and off-diagonal entries “inside” each square). Two levels of sparsity pattern follow the sparsity pattern of node-node incidence matrix for the graph **(right)** similar receptive fields for the inhomogeneous incidence network (I-LAYER) for the same graph. Here, four unique parameters define the dependence of each output node-edge feature on all the input node-edge feature. Two levels of sparsity pattern reflect the sparsity of the node-edge incidence. In particular each edge is adjacent two exactly two nodes.

complement  $\mathcal{B} = \{0, 1\} - \mathcal{P}$  do not need to be ordered and can be taken to be sets. The summation above has four terms, for pooling over rows, columns, both rows and columns and no pooling at all. In each case we re-broadcast the pooled tensor and multiply with a scalar weight  $a_{\mathcal{P}}$  (before, or after the broadcast). Here,  $a_{\mathcal{P}} \forall \mathcal{P} \in 2^{\{0,1\}}$  identify the unique values in  $\mathbf{A}$ . Fig. 2(right) shows these 4 parameters (as different markers) in a parameter-sharing view of  $\mathbf{A}$ , when we look at the receptive field of each output unit.

**H-LAYER.** For a graph, the linear operator  $\mathbf{B}$  on the H-MATRIX can be expressed as pooling the whole matrix and its diagonal and rebroadcasting the resulting matrices, vectors, or scalars across the whole output matrix and its diagonal whenever feasible:

$$\mathbf{B}\mathbf{X} = \sum_{\mathcal{D}_1, \mathcal{D}_2 \in \text{Part}(2)} \sum_{\substack{\mathcal{P} \subseteq \{0, \dots, |\mathcal{D}_1| - 1\} \\ \mathcal{B} \subseteq \{0, \dots, |\mathcal{D}_2| - 1\}}} b_{\mathcal{B}\mathcal{D}_2\mathcal{P}\mathcal{D}_1} \text{Broadcast}_{\mathcal{B}, \mathcal{D}_2} \text{Pool}_{\mathcal{P}, \mathcal{D}_1} \mathbf{X}, \quad (5)$$

where  $\text{Part}(D)$  is the set of ordered partitions of  $D$  objects. For  $D = 2$ , these are  $\{\{0, 1\}\}, \{\{0\}, \{1\}\}, \{\{1\}, \{0\}\}$ . Each linear operation in (5) first identifies a hyper-diagonal with a particular order over its dimensions, using  $\mathcal{D}_1$ . It then pools a subset of its dimensions identified by  $\mathcal{P} \subseteq \{0, \dots, |\mathcal{D}_1| - 1\}$ . Next we pick another hyper-diagonal using  $\mathcal{D}_2$  and broadcast the value obtained from the pooling to the dimensions of this hyper-diagonal identified by  $\mathcal{B}$ . For a more detailed review of these operations see Appendix B.1. Note that (5) has some redundancies (in favour of simplicity of notation) as some choice of  $\mathcal{D}_1, \mathcal{D}_2$  and  $\mathcal{B}$  perform the same operation. Overall there are 15 unique independent operations whose parameters  $b_{\mathcal{B}\mathcal{D}_2\mathcal{P}\mathcal{D}_1}$  are labeled by the corresponding combination of pool/broadcast operations.

Assuming the graph is undirected, pooling over rows and columns of the H-MATRIX produces the same result; similarly transposing the H-MATRIX has no effect. This additional symmetry, reduces the number of parameters from 15 to 11. Moreover, if we constrain the H-LAYER to maintain this symmetry at its output, this number is reduced to 9. Fig. 2 (left) shows these 9 parameters as they appear in the receptive field of each output unit from a parameter-sharing point-of-view.

### 3.2 Which model is more expressive?

We have seen so far that both I-MATRIX and H-MATRIX representations of a graph can encode the same node and edge features. Here, we show that combined with their corresponding layers they also offer similar expressive power.

**Theorem 3.1** (Equivalence of H-LAYER and I-LAYER for graphs). *Let  $\mathbf{X} \in \mathbb{R}^{N \times N \times K}$  be a dense symmetric H-TENSOR and  $\mathbf{Y} \in \mathbb{R}^{N \times N(N-1)/2 \times 2K}$  the corresponding I-TENSOR. Let the I-LAYER and H-LAYER be the permutation equivariant linear layers of (2) and (5), operating on  $\mathbf{Y}$  and  $\mathbf{X}$  respectively. The following statements hold:*

- (a) *a single I-LAYER spans a subspace of linear features spanned by an H-LAYER,*
- (b) *two I-LAYERS span the same linear feature space as an H-LAYER,*
- (c) *two I-LAYERS (or one H-LAYER) span the maximal linear feature space.*

*proof sketch.* We map I-LAYERS and H-LAYERS to operators on the space of node and edge features, and compare the subspaces they span. While a single H-LAYER spans a 9 dimensional subspace, an I-LAYER generates 8 of these 9 features. The missing feature is the one produced by pooling all edges incident to a given node and (symmetrically) broadcasting these back to edges.

We also derive multiplication rules for pooling/broadcasting operations. These allow us to work with composition of I-LAYERS (and H-LAYERS) and prove that two linear I-LAYERS are enough to span the 9 dimensional subspace of an H-LAYER, and that this subspace is the maximal linear subspace spanned by any number of linear H-LAYERS or I-LAYERS. These arguments extend to directed graphs and 15 parameter H-LAYER model. See Appendix A.1 for a detailed derivation.  $\square$

### 3.3 Experiments

To demonstrate that incidence networks are not only principled in their derivation, but also competitive in performance, we applied them to one of the largest benchmark datasets. For details on dataset, preprocessing, architecture and training procedure, see Appendix D.

Table 2: Mean absolute errors on the QM9 targets. ENN-S2S is the neural message passing of Gilmer et al. (2017) and NMP-EDGE Jørgensen et al. (2018) is its improved variation with edge updates. SCHNET uses a continuous filter convolution operation Schütt et al. (2018).

TARGET MOLECULAR PROPERTY	MESSAGE PASSING			INCIDENCE NET.	
	ENN-S2S	NMP-EDGE	SCHNET	HOM.	INHOM.
$\alpha$ (isotropic polarizability)	0.092	0.077	0.235	<b>0.030</b>	<b>0.033</b>
$C_v$ (heat capacity at 298.15K)	0.040	0.032	0.033	<b>0.028</b>	<b>0.029</b>
G (free energy at 298.15K)	0.019	0.012	0.014	<b>0.008</b>	<b>0.010</b>
H (enthalpy at 298.15K)	0.017	0.011	0.014	<b>0.008</b>	<b>0.010</b>
$\epsilon_{HOMO}$ (energy of highest occupied molecular orbital)	0.043	<b>0.036</b>	0.041	0.089	0.090
$\epsilon_{LUMO}$ (energy of lowest occupied molecular orbital)	0.037	<b>0.030</b>	0.034	0.049	0.052
$\Delta\epsilon$ gap (difference between $\epsilon_{HOMO}$ and $\epsilon_{LUMO}$ )	0.069	<b>0.058</b>	0.063	0.068	0.071
$\mu$ (dipole moment)	0.030	<b>0.029</b>	0.033	0.040	0.060
$\langle R_2 \rangle$ (electronic spatial extent)	0.180	0.072	0.073	<b>0.017</b>	<b>0.017</b>
U (internal energy at 298.15K)	0.019	0.010	0.019	<b>0.007</b>	<b>0.009</b>
$U_0$ (internal energy at 0K)	0.019	<b>0.010</b>	0.014	<b>0.008</b>	<b>0.010</b>
ZPVE (zero point vibrational energy)	0.0015	<b>0.0014</b>	0.0017	0.008	0.009

As a surrogate for the more expensive *Density Function Theory*, many deep models for graphs have been applied to the task of predicting molecular properties (Gilmer et al., 2017; Schütt et al., 2018, 2017; Jørgensen et al., 2018; Morris et al., 2018; Unke & Meuwly, 2019; Kondor et al., 2018); interestingly, all of these are message passing methods. A drawback of a fully-fledged message passing scheme compared to incidence networks is its scalability. However, this is nonissue for QM9 dataset (Ramakrishnan et al., 2014) that contains 133,885 small organic molecules. We use atomic features (including atomic coordinates, atom type and atomic numbers) as node features, and encode distance and bond type as edge features in the graph. I-TENSOR and H-TENSORS of these attributed graphs are input to our incidence networks. For each molecule, 12 target chemical properties are calculated at the B3LYP/6-31G(2df,p) level of quantum chemistry. We perform regression task on



these targets, with the same training-test split as competition<sup>5</sup>, reporting the mean absolute error (MAE) on each target.

Our architecture is a simple stack of I-LAYERS (H-LAYERS) for I-TENSOR (H-TENSOR) representation – e.g.,  $\text{Pool}_{\{0,1\}} \mathbf{A}_\ell (\text{ReLU}(\mathbf{A}_{\ell-1} \dots \text{ReLU}(\mathbf{A}_1 \mathbf{Y})) \dots)$ , where the final layer has a single channel and performs a pooling over the entire I-MATRIX (H-MATRIX), producing a scalar value for the target. The 15 parameter H-LAYER was used for the H-LAYERS. We found that batch-normalization (Ioffe & Szegedy, 2015) to be very effective in accelerating the training of incidence networks. The number of layers and channels-per-layer, as well as the mini-batch size are treated as hyper-parameters.

Table 2 reports previous state-of-the-art, as well as our results using the homogeneous and inhomogeneous incidence networks. Both models match or outperform state-of-the-art in 7/12 targets. The also show a very similar performance despite using very different representations and parameter-sharing schemes, supporting our theoretical analysis regarding the expressiveness of homogeneous and inhomogeneous incidence networks. The best performing homogeneous and inhomogeneous incidence networks reported in Table 2 have comparable total number of parameters.

## 4 Higher Order Geometric Structures

Incidence tensor can represent different types of geometric data; see Fig. 1. Before discussing the equivariant models for these structures, we review one of these representations. For representation of hyper-graph and (abstract) polytope see Appendix C.

**Definition 2** (Abstract Simplicial Complex). *Given a set of vertices  $[N]$ , an abstract simplicial complex  $\Delta \subseteq 2^{[N]}$  is a collection of subsets of  $[N]$ , closed under the operation of taking subsets – that is  $\mathcal{A} \in \Delta$  and  $\mathcal{B} \subset \mathcal{A} \rightarrow \mathcal{B} \in \Delta$ . Each  $\mathcal{A} \in \Delta$  is a face of dimension  $|\mathcal{A}| - 1$ . Zero-dimensional faces are called vertices, and maximal faces are called facets. The dimension of  $\Delta$  is the dimension of its largest facet.*

A zero dimensional simplicial complex is a set of points. Going to one dimension, we get undirected graphs, where faces of rank one are the edges. Similarly mesh is a two dimensional simplicial complex; see Fig. 1(a,b,c).

We may assign  $K$  real-valued attributes to each face of dimension  $d \in [D]$ . The resulting structured data has sparse I-TENSOR and H-TENSOR representations. For zero-dimensional simplicial complexes, I-TENSOR and H-TENSOR are identical and the resulting equivariant layer for sets has two unique parameters (Zaheer et al., 2017). For clarity, here we discuss representation of triangulated mesh; see Appendix C1 for the general case.

I-TENSOR representation of triangulated mesh  $\mathbf{Y} \in \mathbb{R}^{N \times N_e \times N_f \times 3K}$  is a tensor of order four, where  $N, N_e, N_f$  are the number of nodes, edges and faces respectively. The sparsity structure reflects the incidence of nodes, edges and faces in the mesh – e.g., each face is adjacent to exactly three nodes and three edges. Similar to graphs, node, edge and face features are broadcasted across the remaining two dimensions, while preserving the sparsity structure. Assuming  $K$  features for nodes, edges and faces each, this gives a channel of size  $3K$ .

H-TENSOR representation of triangulated mesh is  $\mathbf{X} \in \mathbb{R}^{N \times N \times N \times K}$ , where  $d$ -dimensional hyper-diagonals encode features for  $(d - 1)$ -dimensional faces. In particular, the main diagonal encodes node features. Since an edge is identified by two incident nodes, the diagonal planes (2-dimensional hyper-diagonals) encode the edge features. Finally, face features are encoded by the largest hyper-diagonal, i.e., the remaining elements of the tensor. Note that  $\mathbf{X}$  has more than one diagonal plane of order two, and we need all such hyper-diagonals to be equal and symmetric. This is because they all encode the same information about edges that also have no directionality. We call such H-TENSORS in which all hyper-diagonals of order  $d$  are symmetric and equal *strongly symmetric* tensors.

<sup>5</sup>We were not able to compare our experimental results to (Morris et al., 2018) and the results reported in (Wu et al., 2018) due to their choice of using a larger training split. Moreover, the raw QM9 dataset used by (Morris et al., 2018) contains 133,246 molecules, which has 639 fewer molecules than the dataset used in our experiments.

#### 4.1 Pool & Broadcast Interpretation

Generalizing the graph case, we will define I-LAYERS and H-LAYERS operating on higher order geometric objects using the hyper-pooling and hyper-broadcasting operators defined in Section 3.1. One benefit of this interpretation is the linear-time complexity of the equivariant layers, as we can avoid construction of the tensor  $\mathbf{A}$  or  $\mathbf{B}$ . In particular our interpretation of H-LAYER is novel.

The I-LAYER for a higher order I-TENSOR is simply the generalization of the graph case in (4); we only need to replace the set of subset of rows and columns  $\mathcal{P} \in 2^{\{0,1\}}$  that are used for pooling, with its higher dimensional counterpart  $\mathcal{P} \in 2^{[D]}$ .

The resulting summation has  $2^D$  terms, for pooling over any combination of dimensions, including pooling over all dimensions and no pooling at all (Hartford et al., 2018).

Now, consider an H-TENSOR  $\mathbf{X} \in \mathbb{R}^{N \times \dots \times N \times K}$  of order  $D + 1$ . Here, we have  $D$  dimensions of size  $N$  that index nodes, and one dimension of size  $K$  for features. The H-LAYER  $\mathbf{B}$  can be expressed as a combination of hyper-pooling and hyper-broadcasting: first pool over all hyper-diagonals in all possible ways, and then broadcast the resulting collection of pooled tensors to hyper-diagonals of the output tensor, again in all ways possible. Each unique combination of pooled object and broadcasting target receives its own unique parameter – that is

$$\mathbf{B}\mathbf{X} = \sum_{\mathcal{D}_1, \mathcal{D}_2 \in \text{Part}(D)} \sum_{\substack{\mathcal{P} \subseteq \{0, \dots, |\mathcal{D}_1| - 1\} \\ \mathcal{B} \subseteq \{0, \dots, |\mathcal{D}_2| - 1\}}} b_{\mathcal{B}\mathcal{D}_2\mathcal{P}\mathcal{D}_1} \text{Broadcast}_{\mathcal{B}, \mathcal{D}_2} \text{Pool}_{\mathcal{P}, \mathcal{D}_1} \mathbf{X}, \quad (6)$$

where  $\text{Part}(D)$  is the set of ordered partitions of  $D$  elements. (6) is the higher order generalization of (5). Here,  $\mathcal{D}_1$  identifies a hyper-diagonal of order  $m = |\mathcal{D}_1|$  in  $\mathbf{X}$ , and  $\mathcal{P}$  specifies a subset of its dimensions to pool, resulting in a tensor of order  $d = |\mathcal{D}_1| - |\mathcal{P}|$ . This tensor can be broadcasted to any hyper-diagonal of the output tensor with dimension  $m' \geq d$ . This target hyper-diagonal is identified by  $\mathcal{D}_2$  with  $|\mathcal{D}_2| = m'$ .  $\mathcal{B}$  with  $|\mathcal{B}| = d$  then defines the broadcasting operation to this target hyper-diagonal. Counting the number of unique parameters  $b_{\mathcal{B}\mathcal{D}_2\mathcal{P}\mathcal{D}_1}$ , we recover the result of (Maron et al., 2018).

**Claim 1.** *The number of independent operations (i.e., unique parameters) in (6) is  $\text{Bell}(2D)$ , the number of different partitions of a set of size  $2D$ .*

**Strongly symmetric input & output.** In many interesting cases (e.g., triangulated mesh) the input is a strongly symmetric H-TENSOR and we can substantially reduce the complexity of the H-LAYER by constraining the output to be strongly symmetric as well. This is analogous to the 9-parameter H-LAYER for graphs. For triangulated mesh, this reduces the number of parameters from 203 to 23. For each symmetric tensor hyper-pooled from  $\mathbf{X}$ , we can restore the strong symmetry of the output by tying together the parameters associated with all targets that are hyper-diagonals of a given dimension. Next we count these operations.

**Claim 2.** *For strongly symmetric input and output, the number of independent unique parameters in (6) is  $\frac{1}{6}(2D^3 + 9D^2 + D)$ .*

See Appendix A3 and A4 for a derivation of Claim 1 and Claim 2. We also count independent operations for the mixed case symmetric input & unrestricted output in Appendix B2.

#### 4.2 Expressiveness

**Theorem 4.1** (H-LAYERS and I-LAYERS for higher order geometric structures). *Let  $\mathbf{X} \in \mathbb{R}^{N \times \dots \times N \times K}$  be a dense strongly symmetric H-TENSOR of order  $D$ , and  $\mathbf{Y} \in \mathbb{R}^{N \times N_1 \times \dots \times N_{D-1} \times DK}$  the corresponding I-TENSOR, where  $N_d$  is the number of unique elements of dimension  $d$ . Let an H-LAYER be a permutation equivariant layer acting on  $\mathbf{X}$  that preserves the strong symmetry,*



and let an I-LAYER be the permutation equivariant layer acting on  $\mathbf{Y}$ . Then, two I-LAYERS span a superspace of the linear feature space spanned by an arbitrary number of H-LAYERS.

*proof sketch.* For this proof, we generalize the proof technique used for Theorem 3.1.

Using composition rules for pooling/broadcasting operators we prove that, in analogy with the graph case, two I-LAYERS recover at least the full subspace of features generated by one (or an arbitrary number) of H-LAYERS. Unlike the graph case, we show that already a single I-LAYER generates features that cannot be generated by an H-LAYER. For example, for  $D = 3$ , I-LAYERS generate node-triangle features, *i.e.*, features associated with node-triangular face pairs, that are not simply linear combinations of node and triangle features generated by an H-LAYER. See Appendix A.5 for a detailed derivation.  $\square$

## Conclusion

A general approach to learning equivariant models for a family of structured data is through their incidence tensors. We show that such a representation comes in two flavours: homogeneous H-TENSOR, and inhomogeneous I-TENSOR. Their corresponding equivariant linear layers, H-LAYER and I-LAYER—as the building-blocks of deep incidence networks—are non-trivially related: we prove that two or more I-LAYERS applied to an I-TENSOR representation is *at least* as expressive as one or more H-LAYERS, applied to H-TENSOR representation of the same structured data. While for graphs the two are equally expressive, for higher dimensional geometric objects, such as mesh data, the inhomogeneous model is more expressive and more practical at the same time. Empirically, we show that incidence networks achieve state-of-the-art in quantum chemistry tasks. Motivated by these results, we plan to apply incidence networks to higher-dimensional geometric structures in the future.

## References

- Battaglia, P. W., Hamrick, J. B., Bapst, V., Sanchez-Gonzalez, A., Zambaldi, V., Malinowski, M., Tacchetti, A., Raposo, D., Santoro, A., Faulkner, R., et al. Relational inductive biases, deep learning, and graph networks. *arXiv preprint arXiv:1806.01261*, 2018.
- Bronstein, M. M., Bruna, J., LeCun, Y., Szlam, A., and Vandergheynst, P. Geometric deep learning: going beyond euclidean data. *IEEE Signal Processing Magazine*, 34(4):18–42, 2017.
- Bruna, J., Zaremba, W., Szlam, A., and LeCun, Y. Spectral networks and locally connected networks on graphs. *ICLR*, 2014.
- Defferrard, M., Bresson, X., and Vandergheynst, P. Convolutional neural networks on graphs with fast localized spectral filtering. In *Advances in Neural Information Processing Systems*, pp. 3844–3852, 2016.
- Duvenaud, D. K., Maclaurin, D., Iparraguirre, J., Bombarell, R., Hirzel, T., Aspuru-Guzik, A., and Adams, R. P. Convolutional networks on graphs for learning molecular fingerprints. In *Advances in neural information processing systems*, 2015.
- Gilmer, J., Schoenholz, S. S., Riley, P. F., Vinyals, O., and Dahl, G. E. Neural message passing for quantum chemistry. *arXiv preprint arXiv:1704.01212*, 2017.
- Graham, D. and Ravanbakhsh, S. Deep models for relational databases. *arXiv preprint arXiv:1903.09033*, 2019.
- Hamilton, W. L., Ying, R., and Leskovec, J. Representation learning on graphs: Methods and applications. *arXiv preprint arXiv:1709.05584*, 2017.
- Hartford, J., Graham, D. R., Leyton-Brown, K., and Ravanbakhsh, S. Deep models of interactions across sets. In *Proceedings of the 35th International Conference on Machine Learning*, pp. 1909–1918, 2018.
- Henaff, M., Bruna, J., and LeCun, Y. Deep convolutional networks on graph-structured data. *arXiv preprint arXiv:1506.05163*, 2015.

- Ioffe, S. and Szegedy, C. Batch normalization: Accelerating deep network training by reducing internal covariate shift. *arXiv preprint arXiv:1502.03167*, 2015.
- Jørgensen, P. B., Jacobsen, K. W., and Schmidt, M. N. Neural message passing with edge updates for predicting properties of molecules and materials. *arXiv preprint arXiv:1806.03146*, 2018.
- Kearnes, S., McCloskey, K., Berndl, M., Pande, V., and Riley, P. Molecular graph convolutions: moving beyond fingerprints. *Journal of computer-aided molecular design*, 30(8):595–608, 2016.
- Kingma, D. P. and Ba, J. Adam: A method for stochastic optimization. *arXiv preprint arXiv:1412.6980*, 2014.
- Kipf, T. N. and Welling, M. Semi-supervised classification with graph convolutional networks. *arXiv preprint arXiv:1609.02907*, 2016.
- Kondor, R., Son, H. T., Pan, H., Anderson, B., and Trivedi, S. Covariant compositional networks for learning graphs. *arXiv preprint arXiv:1801.02144*, 2018.
- Li, Y., Tarlow, D., Brockschmidt, M., and Zemel, R. Gated graph sequence neural networks. *arXiv preprint arXiv:1511.05493*, 2015.
- Maron, H., Ben-Hamu, H., Shamir, N., and Lipman, Y. Invariant and equivariant graph networks. *arXiv preprint arXiv:1812.09902*, 2018.
- Maron, H., Fetaya, E., Segol, N., and Lipman, Y. On the universality of invariant networks. *arXiv preprint arXiv:1901.09342*, 2019.
- Morris, C., Ritzert, M., Fey, M., Hamilton, W. L., Lenssen, J. E., Rattan, G., and Grohe, M. Weisfeiler and leman go neural: Higher-order graph neural networks. *arXiv preprint arXiv:1810.02244*, 2018.
- Ramakrishnan, R., Dral, P. O., Rupp, M., and Von Lilienfeld, O. A. *Scientific data*, 1:140022, 2014.
- Ravanbakhsh, S., Schneider, J., and Poczos, B. Equivariance through parameter-sharing. In *Proceedings of the 34th International Conference on Machine Learning*, volume 70 of *JMLR: WCP*, August 2017.
- Scarselli, F., Gori, M., Tsoi, A. C., Hagenbuchner, M., and Monfardini, G. The graph neural network model. *IEEE Transactions on Neural Networks*, 20(1):61–80, 2009.
- Schütt, K. T., Arbabzadah, F., Chmiela, S., Müller, K. R., and Tkatchenko, A. Quantum-chemical insights from deep tensor neural networks. *Nature communications*, 8:13890, 2017.
- Schütt, K. T., Sauceda, H. E., Kindermans, P.-J., Tkatchenko, A., and Müller, K.-R. Schnet—a deep learning architecture for molecules and materials. *The Journal of Chemical Physics*, 148(24): 241722, 2018.
- Unke, O. T. and Meuwly, M. Physnet: A neural network for predicting energies, forces, dipole moments and partial charges. *arXiv preprint arXiv:1902.08408*, 2019.
- Wu, Z., Ramsundar, B., Feinberg, E. N., Gomes, J., Geniesse, C., Pappu, A. S., Leswing, K., and Pande, V. Moleculenet: a benchmark for molecular machine learning. *Chemical science*, 9(2): 513–530, 2018.
- Zaheer, M., Kottur, S., Ravanbakhsh, S., Poczos, B., Salakhutdinov, R. R., and Smola, A. J. Deep sets. In *Advances in Neural Information Processing Systems*, 2017.

## A Proofs

### A.1 Proof of Theorem 3.1

In the following (with some abuse of notation) we use the I-LAYER map  $\mathbf{A} : \mathbf{Y} \mapsto \mathbf{Y}'$  also to denote the matrix that maps the vector  $\text{vec}(\mathbf{Y})$  to  $\text{vec}(\mathbf{Y}')$  – that is  $\text{vec}(\mathbf{Y}') = \mathbf{A} \text{vec}(\mathbf{Y})$ . The same notation is used for the H-TENSOR  $\mathbf{X}$  and H-LAYER  $\mathbf{B}$ .

Let  $N_e = N(N-1)/2$  be the number of edges for a complete undirected graph with  $N$  nodes, and  $N_G = N + N_e = N(N+1)/2$  the total number of elements, *i.e.*, the sum of nodes and edges. Also, in the following we will assume a single input-output channel to simplify notation. The proof generalizes to the multi-channel case.

**H-LAYER features.** Recall that the H-MATRIX representation for an undirected graph is a symmetric matrix  $\mathbf{X} \in \mathbb{R}^{N \times N}$ , where diagonal elements encode node features and off-diagonal elements edge features. an H-LAYER returns a matrix  $\mathbf{B}\mathbf{X} = \mathbf{X}' \in \mathbb{R}^{N \times N}$ , so it is natural to interpret diagonal and off-diagonal elements of  $\mathbf{X}'$  as output node and edge features, respectively.

**I-LAYER features.** The I-MATRIX associated with an undirected graph  $\mathbf{Y} \in \mathbb{R}^{N \times N_e \times 2}$  has node features mapped on the first channel along the node dimension and broadcasted across the edge dimension. Similarly, edge features are mapped on the second channel along the edge dimension and broadcasted across the node dimension. Additionally,  $\mathbf{Y}$  has a special sparsity pattern so that an edge  $\langle ij \rangle$  is incident only with nodes  $i$  and  $j$ . An I-LAYER returns a matrix  $\mathbf{A}\mathbf{Y} = \mathbf{Y}' \in \mathbb{R}^{N \times N_e \times 2}$ . All four operations of an I-LAYER, when applied to  $\mathbf{Y}$ , return linear combinations of features that vary at most across one dimension, and are repeated across the remaining dimensions. This is the same pattern of input node and edge features, and we will use the same scheme to interpret them. In particular,

- an output feature that varies across the node dimension (but it is repeated across the edge dimension) is a node feature,
- an output feature that varies across the edge dimension (but it is repeated across the node dimension) is an edge feature,
- and finally a feature that is repeated across both node and edge dimension is either a node or edge feature.

For example, consider a complete graph with three nodes and I-MATRIX given by

$$\mathbf{Y} = \begin{matrix} & \begin{matrix} \langle 12 \rangle & \langle 13 \rangle & \langle 23 \rangle \end{matrix} \\ \begin{matrix} 1 \\ 2 \\ 3 \end{matrix} & \begin{pmatrix} (\eta_1, \boxed{\varepsilon_{12}}) & (\eta_1, \boxed{\varepsilon_{13}}) & - \\ (\boxed{\eta_2}, \varepsilon_{12}) & - & (\eta_2, \boxed{\varepsilon_{23}}) \\ - & (\boxed{\eta_3}, \varepsilon_{13}) & (\eta_3, \varepsilon_{23}) \end{pmatrix} \end{matrix} \quad \begin{matrix} \boxed{\phantom{x}} = \text{edge features} \\ \bigcirc = \text{node features.} \end{matrix} \quad (7)$$

Consider pooling and broadcasting across the edge dimension. Node features were broadcasted across it, and since every node is incident with two edges, we get back multiples of the original features. The edge channel will instead return new features that combine the edges incident on each node. These new node features vary across the node dimension and are broadcasted across the edge dimension,

$$\begin{matrix} & \begin{matrix} \langle 12 \rangle & \langle 13 \rangle & \langle 23 \rangle \end{matrix} \\ \begin{matrix} 1 \\ 2 \\ 3 \end{matrix} & \begin{pmatrix} (2\eta_1, \bigcirc{\varepsilon_{12} + \varepsilon_{13}}) & (2\eta_1, \varepsilon_{12} + \varepsilon_{13}) & - \\ (2\eta_2, \bigcirc{\varepsilon_{12} + \varepsilon_{23}}) & - & (2\eta_2, \varepsilon_{12} + \varepsilon_{23}) \\ - & (2\eta_3, \bigcirc{\varepsilon_{13} + \varepsilon_{23}}) & (2\eta_3, \varepsilon_{13} + \varepsilon_{23}) \end{pmatrix} \end{matrix} \quad (8)$$

On the other hand, pooling and broadcasting across the node dimension returns multiples of input edge features, and generates new edge features from the two nodes incident on each edge,

$$\begin{matrix} & \langle 12 \rangle & \langle 13 \rangle & \langle 23 \rangle \\ \begin{matrix} 1 \\ 2 \\ 3 \end{matrix} & \begin{pmatrix} \boxed{\eta_1 + \eta_2}, 2\varepsilon_{12} & \boxed{\eta_1 + \eta_3}, 2\varepsilon_{13} & - \\ (\eta_1 + \eta_2, 2\varepsilon_{12}) & - & \boxed{\eta_2 + \eta_3}, 2\varepsilon_{23} \\ - & (\eta_1 + \eta_3, 2\varepsilon_{13}) & (\eta_2 + \eta_3, 2\varepsilon_{23}) \end{pmatrix} \end{matrix}. \quad (9)$$

#### A.1.1 Proof of statement (a)

Given the feature encoding described in the previous section, an H-LAYER or an I-LAYER can be represented as a linear function acting on the space of node and edge features,

$$\mathbf{L} : \mathbb{R}^{N_G} \mapsto \mathbb{R}^{N_G}, \quad (10)$$

where  $N_G = N(N+1)/2$  is the number of graph elements, *i.e.*, the sum of nodes and edges. Let us fix a basis in  $\mathbb{R}^{N_G}$  such that the first  $N$  components of a vector  $\phi \in \mathbb{R}^{N_G}$  represent node features and the remaining  $N_e = N(N-1)/2$  represent edge features

$$\phi = \left( \underbrace{\eta_1, \dots, \eta_N}_{\text{node features}}, \underbrace{\varepsilon_1, \dots, \varepsilon_{N_e}}_{\text{edge features}} \right)^\top \equiv (\boldsymbol{\eta}, \boldsymbol{\varepsilon})^\top. \quad (11)$$

Then the layer has a matrix representation  $\mathbf{L} \in \mathbb{R}^{N_G \times N_G}$ ,

$$\phi \mapsto \mathbf{L}\phi = \begin{pmatrix} \mathbf{L}_{\langle nn \rangle} & \mathbf{L}_{\langle ne \rangle} \\ \mathbf{L}_{\langle en \rangle} & \mathbf{L}_{\langle ee \rangle} \end{pmatrix} \begin{pmatrix} \boldsymbol{\eta} \\ \boldsymbol{\varepsilon} \end{pmatrix}, \quad (12)$$

where we have split the matrix into four sub-blocks acting on the sub-vectors of node and edge features. In particular, they represents the following classes of operators:  $\mathbf{L}_{\langle nn \rangle} \in \mathbb{R}^{N \times N}$  maps input node features to output node features,  $\mathbf{L}_{\langle ne \rangle} \in \mathbb{R}^{N \times N_e}$  maps input edge features to output node features,  $\mathbf{L}_{\langle en \rangle} \in \mathbb{R}^{N_e \times N}$  maps input node features to output edge features, and  $\mathbf{L}_{\langle ee \rangle} \in \mathbb{R}^{N_e \times N_e}$  maps input edge features to output edge features.

We write an H-LAYER as

$$\mathbf{B} \simeq \begin{pmatrix} \mathbf{L}_{\langle nn \rangle,0} + \mathbf{L}_{\langle nn \rangle,1} & \mathbf{L}_{\langle ne \rangle,0} + \mathbf{L}_{\langle ne \rangle,1} \\ \mathbf{L}_{\langle en \rangle,0} + \mathbf{L}_{\langle en \rangle,1} & \mathbf{L}_{\langle ee \rangle,0} + \mathbf{L}_{\langle ee \rangle,1} + \mathbf{L}_{\langle ee \rangle,2} \end{pmatrix}, \quad (13)$$

where we have indicated the nine independent operations for an H-LAYER which we summarized in Table 3. We have split the operations according to the sub-blocks defined above, with  $\mathbf{L}_{\langle ab \rangle, i}$  labeling the operator that maps input  $b$  features into output  $a$  features (with  $a$  and  $b$  labeling either node or edges), and with  $i$  representing the dimension of the hyper-pooled tensor. For example,  $\mathbf{L}_{\langle nn \rangle,0}$  is the operator that pools all node features (*i.e.*, it pools the vector of node features to dimension zero) and broadcasts the pooled tensor over nodes. The symbol  $\simeq$  indicates that each operator is defined up to a multiplicative constant (*i.e.*, the corresponding learnable weight  $b$  in (3)). The action of  $\mathbf{B}$  on the space of node and edge features can be uniquely identified by the nine-dimensional subspace

$$\mathbb{V}_{\mathbf{B}} = \text{span} \left\{ \begin{pmatrix} \mathbf{L}_{\langle nn \rangle,0} & 0 \\ 0 & 0 \end{pmatrix}, \begin{pmatrix} \mathbf{L}_{\langle nn \rangle,1} & 0 \\ 0 & 0 \end{pmatrix}, \dots, \begin{pmatrix} 0 & 0 \\ 0 & \mathbf{L}_{\langle ee \rangle,2} \end{pmatrix} \right\} \subseteq \mathbb{R}^{N_G \times N_G}. \quad (14)$$

On the other hand, the four operations on the two channels of an I-LAYER can be mapped to

$$\begin{aligned} \mathbf{A} &\simeq \underbrace{\begin{pmatrix} \mathbf{L}_{\langle nn \rangle,1} & 0 \\ 0 & \mathbf{L}_{\langle ee \rangle,2} \end{pmatrix}}_{\text{identity}} + \underbrace{\begin{pmatrix} \mathbf{L}_{\langle nn \rangle,1} & \mathbf{L}_{\langle ne \rangle,1} \\ 0 & 0 \end{pmatrix}}_{\text{pool/broadcast edges}} + \underbrace{\begin{pmatrix} 0 & 0 \\ \mathbf{L}_{\langle en \rangle,1} & \mathbf{L}_{\langle ee \rangle,2} \end{pmatrix}}_{\text{pool/broadcast nodes}} + \underbrace{\begin{pmatrix} \mathbf{L}_{\langle nn \rangle,0} & \mathbf{L}_{\langle ne \rangle,0} \\ \mathbf{L}_{\langle en \rangle,0} & \mathbf{L}_{\langle ee \rangle,0} \end{pmatrix}}_{\text{pool/broadcast all}} \\ &\simeq \begin{pmatrix} \mathbf{L}_{\langle nn \rangle,0} + \mathbf{L}_{\langle nn \rangle,1} & \mathbf{L}_{\langle ne \rangle,0} + \mathbf{L}_{\langle ne \rangle,1} \\ \mathbf{L}_{\langle en \rangle,0} + \mathbf{L}_{\langle en \rangle,1} & \mathbf{L}_{\langle ee \rangle,0} + \mathbf{L}_{\langle ee \rangle,2} \end{pmatrix}. \end{aligned} \quad (15)$$

In particular,

POOLED FEATURES / BROADCAST TO	NODES	EDGES
EDGES	-	$\mathbf{L}_{\langle ee \rangle, 2}$
NODES	$\mathbf{L}_{\langle nn \rangle, 1}$	$\mathbf{L}_{\langle en \rangle, 1}$
PARTIALLY-POOLED EDGES	$\mathbf{L}_{\langle ne \rangle, 1}$	$\mathbf{L}_{\langle ee \rangle, 1}$
POOLED NODES	$\mathbf{L}_{\langle nn \rangle, 0}$	$\mathbf{L}_{\langle en \rangle, 0}$
POOLED EDGES	$\mathbf{L}_{\langle ne \rangle, 0}$	$\mathbf{L}_{\langle ee \rangle, 0}$

Table 3: The nine operators of an H-LAYER for an undirected graph. Given the pooling/broadcasting definitions of Section 3.1 and the encoding of node and edge features described in Appendix A.1, layer operations can be represented as linear transformations on the space of node and edge features. An operator  $\mathbf{L}_{\langle ab \rangle, i}$  maps input  $b$  features into output  $a$  features (with  $a$  and  $b$  labeling either node or edges), and with  $i$  representing the dimension of the pooled features tensor. Rows represent the pooled features, and columns the hyper-diagonals each row is being broadcasted to. PARTIALLY-POOLED EDGES corresponds to pooling the H-TENSOR  $\mathbf{X}$  (ignoring its diagonal) either across rows or columns. POOLED NODES and POOLED EDGES corresponds to pooling over all node and edge features, respectively.

- identity: if no pooling is applied, we simply map input node and edge features into output node and edge features, respectively. Note that, since we map two input channels into two output channels, we have four independent parameters associated with this operation, but two of them are redundant.
- pool/broadcast edges: when pooling and broadcasting over the edge dimension we are mapping input edge features into output node features, like the example in (8). Input node features are also mapped into (multiples of) themselves. Similarly to the previous case, two of the four parameters are redundant.
- pool/broadcast nodes: when pooling and broadcasting over the node dimension we are mapping input node features into output edge features, like the example in (9). Input edge features are also mapped into (multiples of) themselves. Similarly to the previous case, two of the four parameters are redundant.
- pool/broadcast all: when pooling and broadcasting over both dimensions we get the pooled node and pooled edge features across the entire matrix, which we can interpret as either node or edge features as described in the previous paragraph. We can use the four independent parameters associated with this operation to identify it with the operators that map pooled nodes to node and edges, and pooled edges to node and edges.

From (15), a single I-LAYER does not generate  $\mathbf{L}_{\langle ee \rangle, 1}$ , which corresponds to pooling the original matrix  $\mathbf{X}$  (ignoring the diagonal) to its side and rebroadcasting that to the full matrix (in order to preserve symmetry, the pooled one-dimensional tensor has to be rebroadcasted both across rows and columns). Thus, the subspace  $\mathbb{V}_I \subseteq \mathbb{R}^{N_G \times N_G}$  spanned by an I-LAYER is a subspace of  $\mathbb{V}_H$ ,

$$\mathbb{V}_I = \mathbb{V}_H / \text{span} \left\{ \begin{pmatrix} 0 & 0 \\ 0 & \mathbf{L}_{\langle ee \rangle, 1} \end{pmatrix} \right\} \subset \mathbb{V}_H. \quad (16)$$

### A.1.2 Proof of statements (b) and (c)

Table 4 and Table 5 collect results for the composition of operators defined in Table 3. It is straightforward to derive these results from the definition of the operators. As an example, consider the composition of the two maps  $\mathbf{L}_{\langle ne \rangle, 1} \mathbf{L}_{\langle en \rangle, 1}$ . Here,  $\mathbf{L}_{\langle en \rangle, 1}$  is the operator that broadcasts node features to edge features, it corresponds to taking the diagonal of the  $\mathbf{X}$  matrix, broadcasting it across rows and columns, and summing the results (to restore symmetry). Its domain is node features  $\boldsymbol{\eta}$  and its range is edge features  $\boldsymbol{\varepsilon}$ . On the other hand,  $\mathbf{L}_{\langle ne \rangle, 1}$  pools edge features to one dimension and broadcasts them to nodes. It corresponds to pooling the  $\mathbf{X}$  matrix (ignoring the diagonal) across either rows or columns and broadcasting the result to the diagonal of  $\mathbf{X}$ . This composition has an

	$\mathbf{L}_{\langle nn \rangle,0}$	$\mathbf{L}_{\langle nn \rangle,1}$	$\mathbf{L}_{\langle ne \rangle,0}$	$\mathbf{L}_{\langle ne \rangle,1}$
$\mathbf{L}_{\langle nn \rangle,0}$	$\mathbf{L}_{\langle nn \rangle,0}$	$\mathbf{L}_{\langle nn \rangle,0}$	$\mathbf{L}_{\langle ne \rangle,0}$	$\mathbf{L}_{\langle ne \rangle,0}$
$\mathbf{L}_{\langle nn \rangle,1}$	$\mathbf{L}_{\langle nn \rangle,0}$	$\mathbf{L}_{\langle nn \rangle,1}$	$\mathbf{L}_{\langle ne \rangle,0}$	$\mathbf{L}_{\langle ne \rangle,1}$
$\mathbf{L}_{\langle en \rangle,0}$	$\mathbf{L}_{\langle en \rangle,0}$	$\mathbf{L}_{\langle en \rangle,0}$	$\mathbf{L}_{\langle ee \rangle,0}$	$\mathbf{L}_{\langle ee \rangle,0}$
$\mathbf{L}_{\langle en \rangle,1}$	$\mathbf{L}_{\langle en \rangle,0}$	$\mathbf{L}_{\langle en \rangle,1}$	$\mathbf{L}_{\langle ee \rangle,0}$	$\mathbf{L}_{\langle ee \rangle,1}$

Table 4: Multiplication table for operators defined in Table 3. Here we report multiplications of the type  $\mathbf{L}_{\langle an \rangle,i} \mathbf{L}_{\langle nb \rangle,j}$  with  $n$  labeling nodes, and  $a$  and  $b$  labeling either nodes or edges. Columns should be applied first, *e.g.*, the entry at row  $\mathbf{L}_{\langle nn \rangle,0}$  and column  $\mathbf{L}_{\langle nn \rangle,1}$  means  $\mathbf{L}_{\langle nn \rangle,0} (\mathbf{L}_{\langle nn \rangle,1} \boldsymbol{\eta}) \simeq \mathbf{L}_{\langle nn \rangle,0} \boldsymbol{\eta}$ , where  $\boldsymbol{\eta}$  represents node features. The symbol  $\simeq$  indicates that all operators are defined up to a multiplicative constant. These composition rules can be derived from the general formula in (26).

	$\mathbf{L}_{\langle en \rangle,0}$	$\mathbf{L}_{\langle en \rangle,1}$	$\mathbf{L}_{\langle ee \rangle,0}$	$\mathbf{L}_{\langle ee \rangle,1}$	$\mathbf{L}_{\langle ee \rangle,2}$
$\mathbf{L}_{\langle ne \rangle,0}$	$\mathbf{L}_{\langle nn \rangle,0}$	$\mathbf{L}_{\langle nn \rangle,0}$	$\mathbf{L}_{\langle ne \rangle,0}$	$\mathbf{L}_{\langle ne \rangle,0}$	$\mathbf{L}_{\langle ne \rangle,0}$
$\mathbf{L}_{\langle ne \rangle,1}$	$\mathbf{L}_{\langle nn \rangle,0}$	$\mathbf{L}_{\langle nn \rangle,0} + \mathbf{L}_{\langle nn \rangle,1}$	$\mathbf{L}_{\langle ne \rangle,0}$	$\mathbf{L}_{\langle ne \rangle,0} + \mathbf{L}_{\langle ne \rangle,1}$	$\mathbf{L}_{\langle ne \rangle,1}$
$\mathbf{L}_{\langle ee \rangle,0}$	$\mathbf{L}_{\langle en \rangle,0}$	$\mathbf{L}_{\langle en \rangle,0}$	$\mathbf{L}_{\langle ee \rangle,0}$	$\mathbf{L}_{\langle ee \rangle,0}$	$\mathbf{L}_{\langle ee \rangle,0}$
$\mathbf{L}_{\langle ee \rangle,1}$	$\mathbf{L}_{\langle en \rangle,0}$	$\mathbf{L}_{\langle en \rangle,0} + \mathbf{L}_{\langle en \rangle,1}$	$\mathbf{L}_{\langle ee \rangle,0}$	$\mathbf{L}_{\langle ee \rangle,0} + \mathbf{L}_{\langle ee \rangle,1}$	$\mathbf{L}_{\langle ee \rangle,1}$
$\mathbf{L}_{\langle ee \rangle,2}$	$\mathbf{L}_{\langle en \rangle,0}$	$\mathbf{L}_{\langle en \rangle,1}$	$\mathbf{L}_{\langle ee \rangle,0}$	$\mathbf{L}_{\langle ee \rangle,1}$	$\mathbf{L}_{\langle ee \rangle,2}$

Table 5: Same as in Table 4 but for multiplications of the type  $\mathbf{L}_{\langle ae \rangle,i} \mathbf{L}_{\langle eb \rangle,j}$  with  $e$  labeling edges, and  $a$  and  $b$  labeling either nodes or edges.

alternative expression:

$$\begin{aligned}
\mathbf{L}_{\langle ne \rangle,1} \mathbf{L}_{\langle en \rangle,1} \boldsymbol{\eta} &= \mathbf{L}_{\langle ne \rangle,1} (\text{Broadcast}_{\langle 1 \rangle} + \text{Broadcast}_{\langle 0 \rangle}) \boldsymbol{\eta} \\
&= \text{Broadcast}_{\langle 0 \rangle, \{\{0,1\}\}} \text{Pool}_{\langle 1 \rangle} (\text{Broadcast}_{\langle 1 \rangle} + \text{Broadcast}_{\langle 0 \rangle}) \boldsymbol{\eta} \\
&= \text{Broadcast}_{\langle 0 \rangle, \{\{0,1\}\}} \text{Pool}_{\langle 1 \rangle} \text{Broadcast}_{\langle 1 \rangle} \boldsymbol{\eta} \\
&\quad + \text{Broadcast}_{\langle 0 \rangle, \{\{0,1\}\}} \text{Pool}_{\langle 1 \rangle} \text{Broadcast}_{\langle 0 \rangle} \boldsymbol{\eta} \\
&\simeq (\mathbf{L}_{\langle nn \rangle,0} + \mathbf{L}_{\langle nn \rangle,1}) \boldsymbol{\eta}
\end{aligned} \tag{17}$$

where  $\mathbf{L}_{\langle nn \rangle,0}$  is the operator that pools node features and rebroadcast them to nodes, and  $\mathbf{L}_{\langle nn \rangle,1}$  is an identity operator that rebroadcasts node features into node features. As in the previous section,  $\simeq$  indicates that operators are defined up to a multiplicative constant. All results in Table 4 and Table 5 can be derived in a similar way. We also provide a proof for the general multiplication rule for tensors of any order in (26), of which Table 4 and Table 5 are a particular cases.

Using these multiplication rules, we compose two I-LAYERS and find

$$\mathbf{A}^2 \simeq \begin{pmatrix} \mathbf{L}_{\langle nn \rangle,0} + \mathbf{L}_{\langle nn \rangle,1} & \mathbf{L}_{\langle ne \rangle,0} + \mathbf{L}_{\langle ne \rangle,1} \\ \mathbf{L}_{\langle en \rangle,0} + \mathbf{L}_{\langle en \rangle,1} & \mathbf{L}_{\langle ee \rangle,0} + \mathbf{L}_{\langle ee \rangle,1} + \mathbf{L}_{\langle ee \rangle,2} \end{pmatrix} \simeq \mathbf{B} \implies \mathbb{V}_{\mathbf{A}^2} = \mathbb{V}_{\mathbf{B}}. \tag{18}$$

Two I-LAYERS span the same subspace of operators and thus output features as a single H-LAYER. Note from Table 4 that  $\mathbf{L}_{\langle ee \rangle,1}$  missing from a single I-LAYER is generated by composing  $\mathbf{L}_{\langle ee \rangle,1} \simeq \mathbf{L}_{\langle en \rangle,1} \mathbf{L}_{\langle ne \rangle,1}$ , that is edge features are pooled to one dimension and broadcasted to nodes in the first layer through  $\mathbf{L}_{\langle ne \rangle,1}$ , and then re-broadcasted across rows and columns, like all the other node features, in the second layer through  $\mathbf{L}_{\langle en \rangle,1}$ .

Furthermore, using the same multiplication rules, we find that

$$\mathbf{B} \simeq \mathbf{B}^m \simeq \mathbf{A}^{1+m} \quad \forall m \in \mathbb{N} \mid m \geq 1, \tag{19}$$

thus by taking a single H-LAYER or by stacking two linear I-LAYERS we span the maximal (linear) feature space.



### A.1.3 Extension of Theorem 3.1 to Directed Graphs

A non-symmetric  $\mathbf{X}$  represents directed graphs. In this case an H-LAYER consists of fifteen independent operations. In this section, we show that by increasing the number of I-TENSOR channels it is possible to extend the theorem on equivalent expressiveness to the non-symmetric case. In particular, for  $\mathbf{X} \in \mathbb{R}^{N \times N \times K}$  we can encode node and edge features on an I-TENSOR  $\mathbf{Y} \in \mathbb{R}^{N \times N(N-1) \times 6K}$  and generate the full space of features with two permutation equivariant I-LAYERS. As before, we assume a single input/output channel for simplicity of notation.

**Representation.** For symmetric  $\mathbf{X}$ , we encoded node features on a single channel of  $\mathbf{Y}$ , mapping them along the node dimension and broadcasting across the edge dimension. Similarly, we encoded edge features on a second channel, mapping them along the edge dimension of  $\mathbf{Y}$  and broadcasting across the node dimension. We keep the same scheme here but we use a total of six channels (two for node features and four for edge features), with two different sparsity patterns. A node  $i$  is incident with edge  $\langle ij \rangle$  in the first three channels, and with edge  $\langle ji \rangle$  in the last three channels. Thus, each entry of  $\mathbf{Y}$  has only three active channels. We use the first two to represent node and edge features, and the last to represent the transpose edge feature. For example, consider the case of a complete directed graph of size three:

$$\mathbf{X} = \begin{matrix} & \begin{matrix} 1 & 2 & 3 \end{matrix} \\ \begin{matrix} 1 \\ 2 \\ 3 \end{matrix} & \begin{pmatrix} \eta_1 & \varepsilon_{12} & \varepsilon_{13} \\ \varepsilon_{21} & \eta_2 & \varepsilon_{23} \\ \varepsilon_{31} & \varepsilon_{32} & \eta_3 \end{pmatrix} \end{matrix}, \quad (20)$$

where  $\{\eta_i\}$  are node features and  $\{\varepsilon_{ij}\}$  are edge features. With the representation described above, the first three channels of the corresponding I-TENSOR  $\mathbf{Y}_{0\dots 2}$  and the last three  $\mathbf{Y}_{3\dots 5}$  read

$$\mathbf{Y}_{0\dots 2} = \begin{matrix} & \begin{matrix} \langle 12 \rangle & \langle 13 \rangle & \langle 23 \rangle & \langle 21 \rangle & \langle 31 \rangle & \langle 32 \rangle \end{matrix} \\ \begin{matrix} 1 \\ 2 \\ 3 \end{matrix} & \begin{pmatrix} (\eta_1, \varepsilon_{12}, \varepsilon_{21}) & (\eta_1, \varepsilon_{13}, \varepsilon_{31}) & - & - & - & - \\ - & - & (\eta_2, \varepsilon_{23}, \varepsilon_{32}) & (\eta_2, \varepsilon_{21}, \varepsilon_{12}) & - & - \\ - & - & - & - & (\eta_3, \varepsilon_{31}, \varepsilon_{13}) & (\eta_3, \varepsilon_{32}, \varepsilon_{23}) \end{pmatrix} \end{matrix}, \quad (21)$$

$$\mathbf{Y}_{3\dots 5} = \begin{matrix} & \begin{matrix} - & - & - & (\eta_1, \varepsilon_{21}, \varepsilon_{12}) & (\eta_1, \varepsilon_{31}, \varepsilon_{13}) & - \end{matrix} \\ \begin{matrix} 1 \\ 2 \\ 3 \end{matrix} & \begin{pmatrix} (\eta_2, \varepsilon_{12}, \varepsilon_{21}) & - & - & - & - & - \\ - & (\eta_3, \varepsilon_{13}, \varepsilon_{31}) & (\eta_3, \varepsilon_{23}, \varepsilon_{32}) & - & - & (\eta_2, \varepsilon_{32}, \varepsilon_{23}) \\ - & - & - & - & - & - \end{pmatrix} \end{matrix}. \quad (22)$$

**Equivalence of H-LAYERS and I-LAYERS.** Following the same steps described in Appendix A.1, an I-LAYER generates all H-LAYER operations on node and edge features, except those associated with pooling edges to one-dimensional objects and rebroadcasting those to two dimensions. Note that having node and edge features on channels with different sparsity patterns is crucial to generate all H-LAYER features. In particular,

- identity: generates operations that map node features to node features, edge features to edge features, and edge features to transpose edge features,
- pool/broadcast edges: generates operations where edges are pooled independently either across rows or columns and broadcasted to nodes, using four of the two available edge channels (contrast this with the symmetric case where these two operations yield the same features),
- pool/broadcast nodes: generates operations where node features are broadcasted to edges independently either across rows or columns, using the two node channels (contrast this with the symmetric case where only the sum of these two operations is permitted and it is generated on a single node channel),
- pool/broadcast all: like the symmetric case, this generates operations where node and edge features are pooled to zero-dimensional objects are rebroadcasted to nodes and edges,

for a total of eleven operations. The missing four operations correspond to pooling  $\mathbf{X}$  across columns and rows, and rebroadcasting each of these one-dimensional objects to edges either across rows or columns. One can show that these operations are generated by stacking two I-LAYERS, using multiplication rules analog to those in Table 4 and Table 5 and the four available edge channels.

## A.2 Proof of Claim 1

First we state this counting argument in equations and then elaborate in words:

$$n_H(D) = \sum_{d=0}^D \left[ \sum_{m=d}^D \binom{m}{m-d} \left\{ \begin{matrix} D \\ m \end{matrix} \right\} \sum_{m'=d}^D \frac{m'!}{(m'-d)!} \left\{ \begin{matrix} D \\ m' \end{matrix} \right\} \right] \quad (23)$$

$$= \sum_{d=0}^D \sum_{m=d}^D \sum_{m'=d}^D \left[ \left\{ \begin{matrix} m \\ d \end{matrix} \right\} \left\{ \begin{matrix} D \\ m \end{matrix} \right\} \right] \left[ \left\{ \begin{matrix} m' \\ d \end{matrix} \right\} \left\{ \begin{matrix} D \\ m' \end{matrix} \right\} \right] d! = \text{Bell}(2D). \quad (24)$$

First, we extract a tensor of order  $0 \leq d \leq D$  through hyper-pooling. We can do this by extracting a hyper-diagonal of dimension  $d \leq m \leq D$  and pool over  $m-d$  of its indices. There are  $\left\{ \begin{matrix} D \\ m \end{matrix} \right\}$  hyper-diagonals of dimension  $m$  extracted from a tensor of order  $D$ , and there are  $\binom{m}{m-d}$  ways of pooling over  $m-d$  of its indices. Then, we rebroadcast the hyper-pooled tensor of order  $d$  to hyper-diagonals of order  $d \leq m' \leq D$ . There are  $\left\{ \begin{matrix} D \\ m' \end{matrix} \right\}$  hyper-diagonals, and for each one of these there are only  $m'!/(m'-d)!$  unique ways of broadcasting a tensor of order  $d$  on it.

In the last line of (24),  $\text{Bell}(2D)$  is the Bell number and counts the number of unique partitions of a set of size  $2D$ . To see this, first divide  $[2D]$  in half. Next, partition each half into partitions of different sizes ( $0 \leq m, m' \leq d$ ) and choose  $d$  of these partitions from each half and merge them in pairs. The first two terms count the number of ways we can partition each half into  $m$  (or  $m'$ ) partitions and select a subset of size  $d$  among them. The  $d!$  term accounts for different ways in which  $d$  partitions can be aligned.

## A.3 Proof of Claim 2

Recall that for each symmetric tensor hyper-pooled from  $\mathbf{X}$ , we can restore the strong symmetry of the output by tying together the parameters associated with all broadcasting to a hyper-diagonal of a given dimension. For a strongly symmetric tensor  $\mathbf{X}$  of order  $D$  there are  $(D - \max(d, 1) + 1)$  unique symmetric tensors of order  $d$  that can be extracted through hyper-pooling, and for each one of these there are  $(D - \max(d, 1) + 1)$  broadcasted tensors, one for each dimension  $d \leq m' \leq D$  (except the case  $d = 0$  which can only be broadcasted to dimensions  $1 \leq m' \leq D$  as there are no zero-dimensional hyper-diagonals). The number of independent operations is given by

$$n_H^{(ss)}(D) = \sum_{d=0}^D (D - \max(d, 1) + 1)^2 = \frac{1}{6} (2D^3 + 9D^2 + D). \quad (25)$$

(25) gives, e.g.,  $n_H^{(ss)}(2) = 9$  as discussed at the end of Section 3.1, and  $n_H^{(ss)}(3) = 23$ .

## A.4 Proof of Theorem 4.1

In the following we will assume a single input-output channel to simplify notation. The proof generalizes to the multi-channel case.

### A.4.1 Multiplication Rule for pool/broadcast Operators

Consider the generalization to arbitrary order of operators defined in Table 3 for undirected graphs. Let  $\mathbf{X} \in \mathbb{R}^{N \times \dots \times N}$  be a strongly symmetric H-TENSOR of order  $D$ , and let  $\mathbf{L}_{(ba),i}$  with  $1 \leq a, b \leq D$  and  $0 \leq i \leq a, b$ , label the operator that pools  $(b-1)$ -dimensional geometric elements (i.e., elements of the  $b$ -dimensional hyper-diagonal of  $\mathbf{X}$ ) to a tensor of order  $i$  and rebroadcasts them to  $(a-1)$ -dimensional elements (i.e., to  $a$ -dimensional hyper-diagonals of  $\mathbf{X}$ ). For example, nodes are zero-dimensional elements and associated with the one-dimensional hyper-diagonal, edges are one-dimensional elements and associated with the two-dimensional hyper-diagonals, and so on. Note that due to the strong symmetry of input, the choice of dimensions and their order for pooling is irrelevant, and only the dimensionality of the pooled tensor ( $i$ ) matters – e.g., pooling over rows and columns of a symmetric matrix produce the same vector. Also, assume that the strong symmetry is preserved at the output.

**Lemma 1.** *The following multiplication rule holds*

$$\mathbf{L}_{(ab),i} \mathbf{L}_{(bc),j} \simeq \sum_{k=\max(0,i+j-b)}^{\min(i,j)} \mathbf{L}_{(ac),k}. \quad (26)$$

The symbol  $\simeq$  indicates that operators are defined up to a multiplicative constant.

*Proof.* Let us first consider the action of a single operator and let  $\mathbf{Z} \in \mathbb{R}^{N \times \dots \times N}$  be a symmetric  $c$ -dimensional hyper-diagonal. The operator  $\mathbf{L}_{\langle bc \rangle, j}$  first pools over  $c - j$  of its indices (which we can choose to be the first  $c - j$  indices, since  $\mathbf{Z}$  is symmetric) and then broadcasts it to elements of a symmetric  $b$ -dimensional hyper-diagonal,

$$\mathbf{L}_{\langle bc \rangle, j} \text{vec}(\mathbf{Z}) = \sum_{\mathcal{P} \in 2^{[b]}, |\mathcal{P}|=j} \text{Broadcast}_{\mathcal{P}} \text{Pool}_{[c-j]} \mathbf{Z} \quad (27)$$

where the summation is over all possible choices of broadcasting of the pooled tensor to a  $b$ -dimensional target tensor. Applying the second operator  $\mathbf{L}_{\langle ab \rangle, i}$  gives

$$\mathbf{L}_{\langle ab \rangle, i} (\mathbf{L}_{\langle bc \rangle, j} \text{vec}(\mathbf{Z})) = \sum_{\mathcal{Q} \in 2^{[a]}, |\mathcal{Q}|=i} \text{Broadcast}_{\mathcal{Q}} \text{Pool}_{[b-i]} (\mathbf{L}_{\langle bc \rangle, j} \text{vec}(\mathbf{Z})) \quad (28)$$

$$= \sum_{\mathcal{Q} \in 2^{[a]}, |\mathcal{Q}|=i} \text{Broadcast}_{\mathcal{Q}} \text{Pool}_{[b-i]} \left( \sum_{\mathcal{P} \in 2^{[b]}, |\mathcal{P}|=j} \text{Broadcast}_{\mathcal{P}} \text{Pool}_{[c-j]} \mathbf{Z} \right) \quad (29)$$

$$\simeq \sum_{k=\max(0, i+j-b)}^{\min(i, j)} \sum_{\mathcal{R} \in 2^{[a]}, |\mathcal{R}|=k} \text{Broadcast}_{\mathcal{R}} \text{Pool}_{[a-k]} \mathbf{Z} \quad (30)$$

$$= \sum_{k=\max(0, i+j-b)}^{\min(i, j)} \mathbf{L}_{\langle ac \rangle, k} \text{vec}(\mathbf{Z}) \quad (31)$$

where the first two lines are simply substituting the definition of these operations. The important step is going from (29) to (30). This step is considering all the pooled tensors that can be created and broadcasting them to the target  $a$ -dimensional tensor. Note that only the dimension of these pooled tensors is important as the constants are irrelevant and absorbed in the  $\simeq$  symbol. In particular, the lowest dimension  $\mathbf{Z}$  is pooled to, is  $\max(0, c - (c - j) - (b - i)) = \max(0, i + j - b)$ .

On the other hand, the maximum dimension  $\mathbf{Z}$  is pooled to is  $\min(i, j)$ .  $\square$

Note that Table 4 and Table 5 can be derived from (26). Also, note that (26) is consistent with the special case  $a = b = i$ . In this case  $\mathbf{L}_{\langle bb \rangle, b} \simeq \mathbf{1}$  is proportional to the identity operator. Consistently, we get  $\mathbf{L}_{\langle bb \rangle, b} \mathbf{L}_{\langle bc \rangle, j} \simeq \sum_{k=\max(0, j)}^{\min(b, j)} \mathbf{L}_{\langle bc \rangle, k} = \mathbf{L}_{\langle bc \rangle, j}$ . The same relation holds for the special case  $b = c = j$ .

#### A.4.2 H-LAYER

We generalize (13) for a strongly symmetric H-TENSOR of arbitrary order  $D$ . Nodes and edges are now replaced by zero to  $D - 1$ -dimensional faces. The matrix representing the H-LAYER  $\mathbf{B}$  can be split into  $D^2$  sub-blocks

$$\mathbf{B}_{ab} \simeq \sum_{i=0}^{\min(a, b)} \mathbf{L}_{\langle ab \rangle, i}, \quad (32)$$

with  $1 \leq a, b \leq D$  and  $\mathbf{L}_{\langle ab \rangle, i}$  defined in the previous section. An H-LAYER of order  $D$  is idempotent. In order to prove this it is sufficient to show that  $\mathbf{B}^2 \simeq \mathbf{B}$ . Using (26) we get

$$\begin{aligned} (\mathbf{B}^2)_{ac} &= \sum_{b=1}^D \mathbf{B}_{ab} \mathbf{B}_{bc} \simeq \sum_{b=1}^D \sum_{i=0}^{\min(a, b)} \sum_{j=0}^{\min(b, c)} \mathbf{L}_{\langle ab \rangle, i} \mathbf{L}_{\langle bc \rangle, j} \\ &\simeq \sum_{k=\max(0, i+j-b)}^{\min(i, j)} \sum_{b=1}^D \sum_{i=0}^{\min(a, b)} \sum_{j=0}^{\min(b, c)} \mathbf{L}_{\langle ac \rangle, k} \simeq \sum_{k=0}^{\min(a, c)} \mathbf{L}_{\langle ac \rangle, k} \simeq \mathbf{B}_{ac}. \end{aligned} \quad (33)$$

To prove the second line, first let us assume  $a \leq c$ . Consider the sums over  $i$  and  $j$ , and the terms corresponding to  $i = j = 0$ , which generate  $\mathbf{L}_{\langle ac \rangle, 0}$  for all values of  $b$ . Next, assume  $b \leq a$  and consider the terms  $i = \min(a, b) = b$  and  $j = \min(b, c) = b$ . Then, the first sum generates all operators  $\mathbf{L}_{\langle ac \rangle, k}$  for  $k \in \{1, \dots, a\}$ . Finally, all other terms in the sum generate redundant terms. The same argument holds if  $c < a$ , where now we focus on the terms corresponding to  $b \leq c$  which generate  $\mathbf{L}_{\langle ac \rangle, k}$  for  $k \in \{1, \dots, c\}$ . Thus, we generate all operators  $\mathbf{L}_{\langle ac \rangle, k}$  for  $k \in \{1, \dots, \min(a, c)\}$ .

#### A.4.3 I-LAYER

We generalize (15) to an I-TENSOR corresponding to a strongly symmetric H-TENSOR of arbitrary order  $D$ . Out of the total  $2^D$  operations, we first select a subset of them, comprised of

- identity,
- pool/broadcast over all dimensions,
- pool/broadcast over  $D - 1$  dimensions.

Note that these are the operations that naturally generate features that vary at most across one dimension, and are broadcasted across the remaining dimensions. Extending the discussion of Appendix A.1 to higher order, these have a natural interpretation as features associated with the dimension they vary across. We discuss the remaining operations later. First, we show that composition of these operations alone is equivalent to an H-LAYER. In analogy to (15), the identity generates  $D$  operators, pool/broadcast over all dimensions generates  $D^2$  operators, and the remaining  $D$  pool/broadcast operations generate each  $D - 1$  new operators, for a total of  $2D^2$ . We get

$$\bar{\mathbf{A}}_{ab} \simeq \mathbf{L}_{\langle ab \rangle, 0} + \mathbf{L}_{\langle ab \rangle, \min(a, b)}, \quad (34)$$

where again  $1 \leq a, b \leq D$  and  $\bar{\mathbf{A}}$  indicates that this is a subset of the operations generated by the full I-LAYER  $\mathbf{A}$ . By comparing this with (32), we find that the missing operations are of the type  $\mathbf{L}_{\langle ab \rangle, i}$  for  $0 < i < \min(a, b)$ . Similarly to the graph case, if we stack two linear I-LAYERS we get

$$(\bar{\mathbf{A}}^2)_{ac} = \sum_{b=1}^D \bar{\mathbf{A}}_{ab} \bar{\mathbf{A}}_{bc} \simeq \mathbf{L}_{\langle ac \rangle, 0} + \sum_{b=1}^D \sum_{k=\max(0, \min(a, b) + \min(b, c) - b)}^{\min(\min(a, b), \min(b, c))} \mathbf{L}_{\langle ac \rangle, k} \simeq \sum_{k=0}^{\min(a, c)} \mathbf{L}_{\langle ac \rangle, k} \simeq \mathbf{B}_{ac}, \quad (35)$$

where we used again (26). (35) shows that two I-LAYERS for arbitrary order tensors span at least the same space as a single H-LAYER. In order to prove the last equality, let us assume first  $a \leq c$ . Then, the terms corresponding to  $b \leq a$  generate all  $\mathbf{L}_{\langle ac \rangle, k}$  for  $k \in \{1, \dots, a\}$ . Similarly, if  $c < a$ , terms corresponding to  $b \leq c$  generate all  $\mathbf{L}_{\langle ac \rangle, k}$  for  $k \in \{1 \dots c\}$ . Thus we generate all operators  $\mathbf{L}_{\langle ac \rangle, k}$  for  $k \in \{1, \dots, \min(a, c)\}$ . All the other terms in the sum generate redundant operators. (35) shows that two I-LAYERS for arbitrary order tensors span at least the same space as a single H-LAYER— *i.e.*,

$$\mathbb{V}_{\mathbf{B}} = \mathbb{V}_{\bar{\mathbf{A}}^2} \subseteq \mathbb{V}_{\mathbf{A}^2}. \quad (36)$$

#### A.4.4 I-LAYER is More Expressive

Our next step is to show that for  $D > 2$ , the remaining operations in the I-LAYER produce new features, therefore  $\mathbb{V}_{\mathbf{B}} \subsetneq \mathbb{V}_{\mathbf{A}^2}$ . We show this for  $D = 3$ , noting that the same argument holds also in higher dimensions. Consider an I-TENSOR representing of a “full” simplicial complex of rank 3. We have  $N$  nodes,  $N_e = N(N - 1)/2$  edges, and  $N_f = N(N - 1)(N - 2)/6$  triangular faces. Node, edge, and triangle features are encoded in  $\mathbf{Y} \in \mathbb{R}^{N \times N_e \times N_f \times 3}$  and we have a total of  $2^3 = 8$  tensor operations.

From the previous section we know that identity, pool/broadcast all dimensions, pool/broadcast node and edge dimensions, pool/broadcast node and triangle dimensions, and pool/broadcast edge and triangle dimensions correspond to operations that map input node, edge, and triangle features into output node, edge, and triangle features, according to (34). We also proved that by stacking two linear I-LAYERS and looking only at the operations specified above, we recover the full set of 23 operations generated by (an arbitrary number of) linear H-LAYERS.

Let us focus now on the remaining operations that leave multiple dimensions un-pooled, namely

- pool/broadcast node dimension,
- pool/broadcast triangle dimension,
- pool/broadcast edge dimension.

The first two operations are redundant with the set of operations described in the previous section. They generate new edge features associated with pooling the two nodes adjacent to each edge, and pooling all triangles each edge is incident with, respectively.

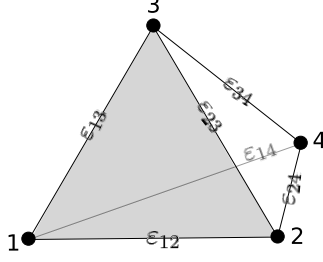


Figure 3: An example of tetrahedron where  $\varepsilon_{ij}$  indicate edge features.

Consider pooling/broadcasting across the edge dimension. Input node and triangle features (*i.e.*, features in the input node and triangle channels) were broadcasted across the edge dimension, thus the operation returns multiples of those. However, features in the input edge channel are now mapped to new features that vary, in general, *both across the node and triangle dimensions*. For each node-triangle pair they correspond to pooling the two edges of the triangle incident with the node. In the following, we show that these are genuine new *node-triangle* features, *i.e.*, they cannot be generated as linear combinations of node and triangle features described in the previous section.

In order to prove this consider the minimal example of a tetrahedron, as in Fig. 3. Let us focus on the new node-triangle features for the three nodes incident with triangle 123 and attempt to write them as a linear combination of node and triangle features. In particular, we are interested in node and triangle features generated from input edge features,

$$\begin{cases} \varepsilon_{12} + \varepsilon_{13} = (a_{\{0,1,2\}}^{11} + a_{\{0,1,2\}}^{22}) \sum_{i < j}^4 \varepsilon_{ij} + a_{\{1,2\}}^{11} \sum_{j=1}^4 \varepsilon_{1j} + a_{\{0,1\}}^{22} \sum_{i < j}^3 \varepsilon_{ij}, \\ \varepsilon_{12} + \varepsilon_{23} = (a_{\{0,1,2\}}^{11} + a_{\{0,1,2\}}^{22}) \sum_{i < j}^4 \varepsilon_{ij} + a_{\{1,2\}}^{11} \sum_{j=2}^4 \varepsilon_{2j} + a_{\{0,1\}}^{22} \sum_{i < j}^3 \varepsilon_{ij}, \\ \varepsilon_{13} + \varepsilon_{23} = (a_{\{0,1,2\}}^{11} + a_{\{0,1,2\}}^{22}) \sum_{i < j}^4 \varepsilon_{ij} + a_{\{1,2\}}^{11} \sum_{j=3}^4 \varepsilon_{3j} + a_{\{0,1\}}^{22} \sum_{i < j}^3 \varepsilon_{ij}, \end{cases} \quad (37)$$

where the left-hand side of each equation is the new node-triangle feature generated for triangle 123 and nodes 1, 2, and 3, respectively. The right-hand side is a linear combination of node and triangle features generated by an I-LAYER. The coefficients  $a_{\mathcal{P}}^{ij}$  are associated with pooling/broadcasting over the set of indices  $\mathcal{P}$ , with  $i, j \in \{0, 1, 2\}$  for the node, edge, and triangle channels. In particular,  $(a_{\{0,1,2\}}^{11} + a_{\{0,1,2\}}^{22})$  are associated with pooling all edges and broadcasting them to node and triangles respectively,  $a_{\{1,2\}}^{11}$  is associated with pooling all edges incident on a node,  $a_{\{0,1\}}^{22}$  is associated with pooling all three edges incident with a triangle. Also, we implemented pooling as sum and assumed  $\varepsilon_{ij} = \varepsilon_{ji}$ . All but the  $a_{\{1,2\}}^{11}$ -terms are common between the three equations, thus by subtracting the second and third from the first equation we get

$$\begin{cases} a_{\{1,2\}}^{11} = \frac{\varepsilon_{13} - \varepsilon_{23}}{\varepsilon_{13} + \varepsilon_{14} - \varepsilon_{23} - \varepsilon_{24}}, \\ a_{\{1,2\}}^{11} = \frac{\varepsilon_{12} - \varepsilon_{23}}{\varepsilon_{12} + \varepsilon_{14} - \varepsilon_{23} - \varepsilon_{34}}, \end{cases} \quad (38)$$

which has no solution for generic values of  $\varepsilon_{ij}$ . The same argument holds with a generic number of nodes. Note that by stacking two I-LAYERS, another triangle feature is generated from pooling all edges incident with the three nodes of a triangle. This feature is also common to all three equations in (37), so the argument is unchanged. This shows that pooling/broadcasting across the edge dimension generates new node-triangle features. Such features are never generated by an H-LAYER, thus proving that an I-LAYER is more expressive than an H-LAYER for strongly symmetric tensors of order  $D = 3$ .

The same proof holds with tensors of any order  $D$ , with the generalization of (37) to include additional features coming from higher-order elements and generated from input edge features. This proves that for strongly symmetric tensors of order  $D \geq 3$  I-LAYERS are more expressive than H-LAYERS.

#### A.4.5 Non-symmetric Case

The setup described for a strongly symmetric tensor applies to a generic tensor of order  $D$ . However the I-TENSOR becomes more complex.

One can generalize the setup described in Appendix A.1.3 for directed graphs, and construct an I-TENSOR with multiple sparsity patterns and a total number of channels given by

$$\alpha(D) = \sum_{d=1}^D \sum_{m=1}^d \sum_{p=m+1}^D \left\{ \begin{matrix} D \\ d \end{matrix} \right\} \binom{d}{m} \binom{p}{m}, \quad (39)$$

where  $\left\{ \begin{matrix} D \\ d \end{matrix} \right\}$  counts the number of hyper-diagonals of dimension  $d$ ,  $\binom{d}{m}$  counts the number of distinct pooled objects of dimension  $m$  we can extract from a hyper-diagonal of dimension  $d$ , and  $\binom{p}{m}$  the number of different ways it can be re-broadcasted to dimension  $p$ . In order to recover at least the set of H-LAYER operations, all these separate configurations need to be encoded on separate channels of the I-TENSOR, and two of them need to be stacked together.

## B Some Remarks on H-LAYER

### B.1 H-LAYER operations for graph

It is useful to review all the pool/broadcast operations:

- When  $\mathcal{D}_1 = \{\{0, 1\}\}$  and  $\mathcal{P} = \{\}$  or  $\{0\}$  hyper-pooling returns the diagonal of  $\mathbf{X}$  or its pooled scalar value, respectively. Each can be broadcasted back to
  - the diagonal  $\mathcal{D}_2 = \{\{0, 1\}\}$ , with  $\mathcal{B} = \langle \rangle, \langle 0 \rangle$  for pooled diagonal and diagonal, respectively and,
  - the whole matrix  $\mathcal{D}_2 = \{\{0\}, \{1\}\}$ , with  $\mathcal{B} = \langle \rangle$  for pooled diagonal, and  $\mathcal{B} = \langle 0 \rangle, \langle 1 \rangle$  for the diagonal.
- When  $\mathcal{D}_1 = \{\{0\}, \{1\}\}$  and  $\mathcal{P} \in 2^{\{0,1\}}$  hyper-pooling returns all possible poolings on the whole matrix (*i.e.*, no pooling at all for  $\mathcal{P} = \{\}$ , pooling across rows for  $\mathcal{P} = \{0\}$ , pooling across columns for  $\mathcal{P} = \{1\}$ , pooling all for  $\mathcal{P} = \{0, 1\}$ ). When applicable, these objects can be rebroadcasted back to
  - the diagonal  $\mathcal{D}_2 = \{\{0, 1\}\}$  with  $\mathcal{B} = \langle \rangle, \langle 0 \rangle$  for zero- and one-dimensional objects respectively,
  - and the whole matrix  $\mathcal{D}_2 = \{\{0\}, \{1\}\}$  with  $\mathcal{B} = \langle \rangle$  for zero-dimensional objects,  $\mathcal{B} = \langle 0 \rangle, \langle 1 \rangle$  for one-dimensional objects, and  $\mathcal{B} = \langle 0, 1 \rangle, \langle 1, 0 \rangle$  for two-dimensional objects.
- The case  $\mathcal{D}_1, \mathcal{D}_2 = \{\{1\}, \{0\}\}$  is redundant as we have already included transpose operations and broadcasting across rows or columns through a proper choice of the ordered indices  $\mathcal{B}$ .

Note that the diagonal and the pooled-matrix across rows and columns can be rebroadcasted to the whole matrix both across rows and columns. Also, note that  $\mathcal{P}$  does not need to be ordered and can be taken to be a set. Overall this amounts to 15 independent operations whose parameters  $b_{\mathcal{B}\mathcal{D}_2\mathcal{P}\mathcal{D}_1}$  are labeled by the corresponding combination of pool/broadcast operations.

### B.2 H-LAYER for strongly symmetric input and unrestricted output

Consider the special case of (6) when  $\mathbf{X}$  is strongly symmetric, *i.e.*, it is symmetric under all  $D!$  permutations of its indices and additionally all its hyper-diagonals of order  $0 < d < D$  are symmetric and equal. In other words, there are exactly  $D$  unique and symmetric hyper-diagonals, including  $\mathbf{X}$  itself. Under these assumptions the total number of independent operations is given by

$$\begin{aligned} n_H^{(s)}(D) &= \sum_{d=0}^D \left[ (D - \max(d, 1) + 1) \sum_{m'=d}^D \binom{m'}{d} \left\{ \begin{matrix} D \\ m' \end{matrix} \right\} \right] \\ &= \sum_{d=1}^D \left[ (D - d + 1) \sum_{m'=d}^D \binom{m'}{d} \left\{ \begin{matrix} D \\ m' \end{matrix} \right\} \right] + D \text{Bell}(D). \end{aligned} \quad (40)$$



In the first line,  $(D - \max(d, 1) + 1)$  counts the number of unique symmetric hyper-pooled tensors of order  $d$ , and  $\sum_{m'=d}^D \binom{m'}{d} \{ \frac{D}{m'} \}$  counts the number of unique broadcastings to hyper-diagonals of dimension  $d \leq m' \leq D$  of the output tensor. Note that broadcasting counting is identical to the broadcasting term in (24), where we have additionally divided by  $d!$  to account for the symmetry of the broadcasted tensor. From (40) we get, e.g.,  $n_H^{(s)}(2) = 11$  and  $n_H^{(s)}(3) = 58$ . Note that the output, in general, will not preserve the symmetry of the input.

## C Details on Representation of Geometric Structures

### C.1 Abstract Simplicial Complex

Given a set of vertices  $[N]$ , an abstract simplicial complex  $\Delta \subseteq 2^{[N]}$  is a collection of subsets of  $[N]$ , closed under the operation of taking subsets – that is  $\mathcal{A} \in \Delta$  and  $\mathcal{B} \subset \mathcal{A} \rightarrow \mathcal{B} \in \Delta$ . Each  $\mathcal{A} \in \Delta$  is a *face* of *dimension*  $|\mathcal{A}| - 1$ . Zero-dimensional faces are called *vertices*, and maximal faces are called *facets*. The dimension of  $\Delta$  is the dimension of its largest facet. If all the facets have the same dimension,  $\Delta$  is called *pure*. Geometric realisation of this structure has a central role in topology, and in particular topological data analysis. The same type of structure represents independence system in Matroid theory.

We may assign  $K$  real-valued attributes to each face of dimension  $d \in [D]$ . The resulting structured data has sparse I-TENSOR and H-TENSOR representations. For concreteness, here we continue the discussion using mesh data; see Appendix C.1 for the general case.

#### C.1.1 I-TENSOR Representation

For this, divide the faces  $\mathcal{A} \in \Delta$ , into subsets of different dimension, and let  $i_d \in [N_d]$  index  $d$ -dimensional faces. We then use  $\mathbf{Y} \in \mathbb{R}^{N_0 \times \dots \times N_{D-1} \times K}$ , to represent the attributed  $\Delta$ . The element  $\mathbf{Y}_{i_0 \dots i_{D-1} i_k}$  is non-zero iff all the faces  $i_0 \dots i_{D-1}$  are incident (note that they all have different dimensions). The  $(K = \sum_d K_d)$ -dimensional feature dimension in  $\mathbf{Y}_{i_0 \dots i_{D-1} i_k}$  is simply the concatenation of features for all these adjacent faces.

#### C.1.2 Symmetry and H-TENSOR Representation

A homogeneous tensor  $\mathbf{X}$  is *symmetric* iff it is invariant to any permutation of its dimensions  $\mathbf{X}_{i_0 \dots i_{D-1} i_k} = \mathbf{X}_{i_{\rho(0)} \dots i_{\rho(D-1)} i_k}$ , where  $\rho \in S^D$ . Note that this is different from permutations applied “within” individual dimension. This notion of symmetry does not guarantee the equality or the symmetry of hyper-diagonals.

We call a tensor  $\mathbf{X}$  *strongly symmetric* iff all order  $d \in [D]$  hyper-diagonals of  $\mathbf{X}$  are equal and symmetric. The appeal of defining a strongly symmetric tensor is that  $d^{\text{th}}$ -order hyper-diagonal represent the symmetric interactions between (or incidence of)  $N$  objects for  $1 \leq d \leq D$ . For example, the first order interactions ( $d = 1$ ) is encoded in the *main diagonal*  $i_0 = \dots = i_{D-1}$ ; these are feature vectors of length  $K$  associated with each of  $N$  objects. Hyper-diagonals of rank two (all being equal and symmetric) represent second order interactions between  $n', n \in [N]$  for  $n \neq n'$ , and so on. For a second order tensor (e.g., node-node incidence matrix), strong symmetry and symmetry are the same conditions.

We can now represent attributed  $\Delta$  using a strongly symmetric H-TENSOR  $\mathbf{X} \in \mathbb{R}^{N \times \dots \times N \times K}$  of order  $D + 1$ . Here  $d$ -dimensional faces are mapped to hyper-diagonals of order  $d + 1$ , and strong symmetry follows from the lack of order in members of  $\Delta$ .

### C.2 Hyper-Graph

Hyper-graphs is a generalization of graph where each edge is adjacent to a set of nodes.<sup>6</sup> The I-TENSOR representation for hyper-graph is similar to I-TENSOR for undirected graphs – that is  $\mathbf{Y} \in \mathbb{R}^{N \times N_e \times K}$ . The only difference with a graph is that in a hyper-graph, each edge is potentially adjacent to more than one nodes. If all hyper-edges have the same degree  $M$ , then one may also represent the hyper-graph using a strongly symmetric H-TENSOR of order  $M$ , where only the

<sup>6</sup>Note that this is different from the definition of (Maron et al., 2018), where hyper-edges assume an order.

main diagonal and the largest hyper-diagonal have non-zero features. This makes I-TENSOR the representation of choice for hyper-graphs.

### C.3 Abstract Polytope

A polytope is a generalization of polygon and polyhedron to higher dimensions. An abstract polytope also generalizes The structure of an abstract polytope is encoded using a graded partially ordered set. A partially ordered set (poset) is set equipped with a partial order that allows certain members to be compared with each other in a transitive way. A poset  $\mathcal{P}$  is graded if there exists a rank function  $\text{rank} : \mathcal{P} \rightarrow \mathbb{N}$  that is compatible with the partial order and for two members  $A, B \in \mathcal{P}$  such that  $A < B$  and  $\nexists C \in \mathcal{P} \text{ s.t. } A < C < B$ ,  $\text{rank}(B) = \text{rank}(A) + 1$ . The abstract simplicial complexes are graded polytopes, where rank and incidence is naturally defined. Another structure that builds on a graded poset is abstract polytope, which is a set of partially ordered faces of different dimension. The partial order is naturally defined by the inclusion of a lower-dimensional face in a higher dimensional one (e.g., an edge that appears in a face of a cube). In a polytope, the empty set has rank  $-1$  and the all maximal faces have dimension  $D - 1$ . A path from  $\emptyset$  to a maximal face is called a *flag*.

I-TENSOR tensors can represent incidence structure in abstract polytopes and more generally graded posets. Here, similar to an abstract simplicial complex, each dimension of  $\mathbf{Y}$  is associated with faces of a particular rank  $d$ , and  $Y_{i_0, \dots, i_{D-1}, i_k}$  is non-zero iff  $i_0, \dots, i_{D-1}$  is a flag. Interestingly one may also represent a hyper-graph using a poset of rank one. The difficulty in using H-TENSOR representation is analogous to the case of hyper-graphs. The problem is only compounded here due to existence of faces of higher dimension.

## D Details on Experiments

QM9 dataset contains 133,885 small organic molecules consist of Hydrogen (H), Carbon (C), Oxygen (O), Nitrogen (N), and Flourine (F) atoms and contain up to 9 heavy (non Hydrogen) atoms and up to 29 atoms in total including Hydrogen. There are a number of features available for each atom in a molecule including atomic coordinates, atom type, atomic numbers, etc. We use all these atomic features as node features in the input graph representation. Moreover, We use edge length (the distance between each two atoms) along with one-hot representation of bond type (single, double, triple, or aromatic) as edge features in the graph. For each molecule, 12 target chemical properties are calculated at the B3LYP/6-31G(2df,p) level of quantum chemistry. We perform regression task on these targets and evaluate mean absolute error.

Following [Gilmer et al. \(2017\)](#), we randomly chose 10000 samples for validation, 10000 samples for testing, and used the rest for training. All targets were normalized to have mean 0 and variance 1. We trained one model per target and performed (non-exhaustive) hyper parameter search for the number of layers  $3 \leq \ell \leq 20$ , channels in  $\{128, 256\}$ , and batch size in  $\{16, 32, 64, 128\}$ . We used ADAM ([Kingma & Ba, 2014](#)) with an initial learning rate of  $10^{-3}$  and adaptive learning rate decay based on validation error. We trained each model for 1000 epochs and minimized the mean squared error between the model output and the target. A small weight decay of  $10^{-6}$  was used. During training, for every molecule in the mini-batch we randomly rotate atom coordinates with uniform distribution along z axis in each epoch.